

A flexible Particle Markov chain Monte Carlo method

Eduardo F. Mendes
School of Applied Mathematics
Fundação Getulio Vargas

Christopher K. Carter
School of Economics
University of New South Wales

David Gunawan
School of Economics
University of New South Wales

Robert Kohn
School of Economics
University of New South Wales

Abstract

Particle Markov Chain Monte Carlo methods are used to carry out inference in non-linear and non-Gaussian state space models, where the posterior density of the states is approximated using particles. Current approaches usually perform Bayesian inference using either a particle Marginal Metropolis-Hastings (PMMH) algorithm or a particle Gibbs (PG) sampler. This paper shows how the two ways of generating variables mentioned above can be combined in a flexible manner to give sampling schemes that converge to a desired target distribution. The advantage of our approach is that the sampling scheme can be tailored to obtain good results for different applications. For example, when some parameters and the states are highly correlated, such parameters can be generated using PMMH, while all other parameters are generated using PG because it is easier to obtain good proposals for the parameters within the PG framework. We derive some convergence properties of our sampling scheme and also investigate its performance empirically by applying it to univariate and multivariate stochastic volatility models and comparing it to other PMCMC methods proposed in the literature.

Keywords: Diffusion equation; Factor stochastic volatility model; Metropolis-Hastings; Particle Gibbs sampler.

1 Introduction

Our article deals with statistical inference for both the unobserved states and the parameters in a class of state space models. Its main goal is to give a flexible approach to constructing sampling schemes that converge to the posterior distribution of the states and the parameters. The sampling schemes generate particles as auxiliary variables. This work extends the methods proposed by Andrieu et al. [2010], Olsson and Ryden [2011], Lindsten and Schön

[2012b], Lindsten et al. [2014], Fearnhead and Meligkotsidou [2016], and Deligiannidis et al. [2018].

Andrieu et al. [2010] introduce two particle Markov chain Monte Carlo (MCMC) methods for state space models. The first is particle marginal Metropolis-Hastings (PMMH), where the parameters are generated with the states integrated out. The second is particle Gibbs (PG), which generates the parameters given the states. They show that the augmented density targeted by this algorithm has the joint posterior density of the parameters and states as a marginal density. Andrieu et al. [2010] and Andrieu and Roberts [2009] show that the law of the marginal sequence of parameters and states, sampled using either PG or PMMH, converges to the true posterior as the number of iterations increase. Both particle MCMC methods are the focus of recent research. Olsson and Ryden [2011] and Lindsten and Schön [2012b] use *backward simulation* [Godsill et al., 2004] for sampling the state vector, instead of *ancestral tracing* [Kitagawa, 1996]. Lindsten and Schön [2012b] extend the PG sampler to a particle Metropolis within Gibbs (PMwG) sampler to deal with the case where the parameters cannot be generated exactly conditional on the states. Fearnhead and Meligkotsidou [2016] proposed an augmented particle MCMC methods. They show that their method can improve the mixing of the particle Gibbs when the parameters are highly correlated with the states. Recently, Deligiannidis et al. [2018] proposed the correlated pseudo marginal Metropolis-Hastings method that significantly reduce the number of particles used by the standard pseudo marginal method. Unless stated otherwise, we write PG to denote both the PG and PMwG samplers that generate the parameters conditional on the states.

We note that there are no formal results in the literature to guide the user on whether to use PMMH or PG for any given problem. Our work extends the particle MCMC framework to situations where using just PMMH or just PG is inefficient. It is well-known from the literature on Gaussian and conditionally Gaussian state space models that confining MCMC for state space models to Gibbs sampling or Metropolis-Hastings sampling can result in inefficient or even degenerate sampling. See, for example, Kim et al. [1998] who show for a stochastic volatility model that generating the states conditional on the parameters and the parameters conditional on the states can result in a highly inefficient sampler. See also Carter and Kohn [1996] and Gerlach et al. [2000] who demonstrate using a signal plus noise model that a Gibbs sampler for the states and indicator variables for the structural breaks produces a degenerate sampler. A natural solution is to combine Gibbs and Metropolis-Hastings samplers. Motivated by that, we derive a particle sampler on the same augmented space as the PMMH and PG samplers, in which some parameters are sampled conditionally on the states and the remaining parameters are sampled with the states integrated out. We call this a PMMH+PG sampler. We show that the PMMH+PG sampler targets the same augmented density as the PMMH or PG samplers. We provide supplementary material showing that the Markov chain generated by the algorithm is uniformly ergodic, given regularity conditions. It implies that the marginal law of the Markov chain generated by n^{th} iteration of the algorithm converges to the posterior density function geometrically fast, uniformly on its starting value, as $n \rightarrow \infty$.

We use *ancestral tracing* in the particle Gibbs step to make the presentation accessible.

The online supplementary material shows how to modify the methods proposed in the paper to incorporate auxiliary particle filters and *backward simulation* in the particle Gibbs step. The same convergence results for the latter methods are obtained by modifying the arguments in Olsson and Ryden [2011].

We apply our PMMH+PG sampler to several univariate and multivariate examples using simulated and real datasets. As a main application we propose a general algorithm for Bayesian inference on a multivariate factor stochastic volatility (SV) model. This model is used to jointly model many co-varying financial time series, as it is able to capture the common features using only a small number of latent factors (see, e.g. Chib et al. [2006] and Kastner et al. [2017]). We consider a factor SV model in which the volatilities of the factors follow a traditional SV model (as in Chib et al. [2006] and Kastner et al. [2017]) and the log-volatilities of the idiosyncratic errors follow either a continuous time Ornstein-Uhlenbeck (OU) process [Stein and Stein, 1991] or a GARCH diffusion process [Chib et al., 2004, Kleppe et al., 2010]. The OU process admits a closed form transition density whereas the GARCH process does not. Similar factor models can also be applied to spatial temporal data with a large number of spatial measurements at each time point.

We use these examples to compare the performance of our sampling schemes to the standard PMMH and PG samplers of Andrieu et al. [2010], the particle Gibbs with data augmentation sampler of Fearnhead and Meligkotsidou [2016], and the correlated PMMH of Deligiannidis et al. [2018]. For the standard and correlated PMMH, we consider adaptive random walk proposals and the refined proposals by Dahlin et al. [2015] and Nemeth et al. [2016b]. We show that the PMMH + PG sampler outperforms these methods in the situation where we have both a large number of parameters and a large number of latent states. In general, there are likely to be a number of different sampling schemes that can solve the same problems addressed in our article, and which sampler is best depends on a number of factors such as the model, the data set and the number of observations. We also note that our PMMH + PG approach can be further refined by using the data augmented PMMH and PG sampling schemes proposed by Fearnhead and Meligkotsidou [2016] and the refined proposals for the PMMH sampling scheme by Dahlin et al. [2015] and Nemeth et al. [2016b].

The rest of the paper is organized as follows. Section 2 introduces the basic concepts and notation used throughout the paper as well as the PMMH+PG sampler for estimating a single state space model and its associated parameters. Sections 3 and 4 compare the performance of the PMMH+PG sampler to other competing PMCMC methods for estimating univariate and multivariate stochastic volatility models, respectively. The paper has an online supplement which contains some further empirical and technical results.

2 The PMMH+PG sampling scheme for state space models

This section introduces a sampling scheme that combines PMMH and PG steps for the Bayesian estimation of a state space model. The first three sections give preliminary results

and Section 2.4 presents the sampling scheme. The methods and models introduced in this section are used in the univariate models in Section 3 and the multivariate models in Section 4.

2.1 State space model

Define \mathbb{N} as the set of positive integers and let $\{X_t\}_{t \in \mathbb{N}}$ and $\{Y_t\}_{t \in \mathbb{N}}$ denote \mathcal{X} -valued and \mathcal{Y} -valued stochastic processes, where $\{X_t\}_{t \in \mathbb{N}}$ is a latent Markov process with initial density $f_1^\theta(x)$ and transition density $f_t^\theta(x'|x)$, i.e.,

$$X_1 \sim f_1^\theta(\cdot) \quad \text{and} \quad X_t | (X_{t-1} = x) \sim f_t^\theta(\cdot | x) \quad (t = 2, 3, \dots).$$

The latent process $\{X_t\}_{t \in \mathbb{N}}$ is observed only through $\{Y_t\}_{t \in \mathbb{N}}$, whose value at time t depends on the value of the hidden state at time t , and is distributed according to $g_t^\theta(y|x)$

$$Y_t | (X_t = x) \sim g_t^\theta(\cdot | x) \quad (t = 1, 2, \dots).$$

The densities f_t^θ and g_t^θ are indexed by a parameter vector $\theta \in \Theta$, where Θ is an open subset of \mathbb{R}^{d_θ} , and all densities are with respect to suitable dominating measures, denoted as dx and dy . The dominating measures are frequently taken to be the Lebesgue measure if $\mathcal{X} \in \mathcal{B}(\mathbb{R}^{d_x})$ and $\mathcal{Y} \in \mathcal{B}(\mathbb{R}^{d_y})$, where $\mathcal{B}(A)$ is the Borel σ -algebra generated by the set A . Usually $\mathcal{X} = \mathbb{R}^{d_x}$ and $\mathcal{Y} = \mathbb{R}^{d_y}$.

We use the colon notation for collections of random variables, i.e., $a_t^{1:N} = (a_t^1, \dots, a_t^N)$ and for $t \leq u$, $a_{t:u}^{1:N} = (a_t^{1:N}, \dots, a_u^{1:N})$. The joint probability density function of $(x_{1:T}, y_{1:T})$ is

$$p(x_{1:T}, y_{1:T} | \theta) = f_1^\theta(x_1) g_1^\theta(y_1 | x_1) \prod_{t=2}^T f_t^\theta(x_t | x_{t-1}) g_t^\theta(y_t | x_t).$$

We define $Z_1(\theta) := p(y_1 | \theta)$ and $Z_t(\theta) := p(y_t | y_{1:t-1}, \theta)$ for $t \geq 2$, so the likelihood is $Z_{1:T}(\theta) = Z_1(\theta) \times Z_2(\theta) \dots Z_T(\theta)$. The joint filtering density of $X_{1:t}$ is

$$p(x_{1:t} | y_{1:t}, \theta) = \frac{p(x_{1:t}, y_{1:t} | \theta)}{Z_{1:t}(\theta)}.$$

The posterior density of θ and $X_{1:T}$ can also be factorized as

$$p(x_{1:T}, \theta | y_{1:T}) = \frac{p(x_{1:T}, y_{1:T} | \theta) p(\theta)}{\bar{Z}_{1:T}},$$

where the marginal likelihood $\bar{Z}_T = \int_{\Theta} Z_{1:T}(\theta) p(\theta) d\theta = p(y_{1:T})$. This factorization is used in the particle Markov chain Monte Carlo algorithms.

2.2 Target distribution for state space models

We first approximate the joint filtering densities $\{p(x_t|y_{1:t}, \theta) : t = 1, 2, \dots\}$ sequentially, using particles, i.e., weighted samples, $(x_t^{1:N}, \bar{w}_t^{1:N})$, drawn from auxiliary distributions m_t^θ . This requires specifying *importance densities* $m_1^\theta(x_1) := m_1(x_1|Y_1 = y_1, \theta)$ and $m_t^\theta(x_t|x_{t-1}) := m_t(x_t|X_{t-1} = x_{t-1}, Y_{1:t} = y_{1:t}, \theta)$, and a resampling scheme $\mathcal{M}(a_{t-1}^{1:N}|\bar{w}_{t-1}^{1:N})$, where each $a_{t-1}^i = k$ indexes a particle in $(x_{t-1}^{1:N}, \bar{w}_{t-1}^{1:N})$, and is sampled with probability \bar{w}_{t-1}^k . We refer to Doucet et al. [2000], Van Der Merwe et al. [2001], and Guo et al. [2005] for the choice of importance densities and Douc and Cappé [2005] for a comparison between resampling schemes. Unless stated otherwise, upper case letters indicate random variables and lower case letters indicate the corresponding values of these random variables, e.g., A_t^j and a_t^j , X_t and x_t . We denote the vector of particles by

$$U_{1:T} := (X_1^{1:N}, \dots, X_T^{1:N}, A_1^{1:N}, \dots, A_{T-1}^{1:N}) \quad (1)$$

where a_t^j is the value of the random variable A_t^j and its sample space by $\mathcal{U} := \mathcal{X}^{TN} \times \mathbb{N}^{(T-1)N}$.

The Sequential Monte Carlo (SMC) algorithm used here is the same one as in Section 4.1 of Andrieu et al. [2010], and is defined in Section S1 and Algorithm S1 in the supplementary material. The algorithm provides an unbiased estimate

$$\widehat{Z}_T(\theta) = Z(u_{1:T}, \theta) := \prod_{t=1}^T \left(N^{-1} \sum_{i=1}^N w_t^i \right),$$

of the likelihood, where

$$w_1^i = \frac{f_1^\theta(x_1^i) g_1^\theta(y_1|x_1^i)}{m_1^\theta(x_1^i)}, w_t^i = \frac{g_t^\theta(y_t|x_t^i) f_t^\theta(x_t^i|x_{t-1}^{a_{t-1}^i})}{m_t^\theta(x_t^i|x_{t-1}^{a_{t-1}^i})} \text{ for } t = 2, \dots, T, \text{ and } \bar{w}_t^i = \frac{w_t^i}{\sum_{j=1}^N w_t^j}.$$

The joint distribution of the particles given the parameters is

$$\psi(u_{1:T}|\theta) := \prod_{i=1}^N m_1^\theta(x_1^i) \prod_{t=2}^T \left\{ \mathcal{M}(a_{t-1}^{1:N}|\bar{w}_{t-1}^{1:N}) \prod_{i=1}^N m_t^\theta(x_t^i|x_{t-1}^{a_{t-1}^i}) \right\}. \quad (2)$$

The key idea of particle MCMC methods is to construct a target distribution on an augmented space that includes the particles $U_{1:T}$ and has a marginal distribution equal to $p(x_{1:T}, \theta|y_{1:T})$. This section describes the target distribution from Andrieu et al. [2010]. Later sections describe particle MCMC methods to sample from this distribution and hence sample from $p(x_{1:T}, \theta|y_{1:T})$. Section S3 of the supplementary material describes other choices of target distribution and how it is straightforward to modify our results to apply to them.

The simplest way of sampling from the particle approximation of $p(x_{1:T}|y_{1:T}, \theta)$ is called *ancestral tracing*. It was introduced in Kitagawa [1996] and used in Andrieu et al. [2010] and consists of sampling one particle from the final particle filter. The method is equivalent to sampling an index $J = j$ with probability \bar{w}_T^j , tracing back its ancestral lineage $b_{1:T}^j$ ($b_T^j = j$ and $b_{t-1}^j = a_{t-1}^{b_t^j}$) and choosing the particle $x_{1:T}^j = (x_1^{b_1^j}, \dots, x_T^{b_T^j})$.

With some abuse of notation, for a vector a_t , denote $a_t^{(-k)} = (a_t^1, \dots, a_t^{k-1}, a_t^{k+1}, \dots, a_t^N)$, with obvious changes for $k \in \{1, N\}$, and denote

$$u_{1:T}^{(-j)} = \left\{ x_1^{(-b_1^j)}, \dots, x_{T-1}^{(-b_{T-1}^j)}, x_T^{(-j)}, a_1^{(-b_1^j)}, \dots, a_{T-1}^{(-b_{T-1}^j)} \right\}.$$

It simplifies the notation to sometimes use the following one-to-one transformation

$$(u_{1:T}, j) \leftrightarrow \left\{ x_{1:T}^j, b_{1:T-1}^j, j, u_{1:T}^{(-j)} \right\},$$

and switch between the two representations and use whichever is more convenient. Note that the right hand expression will sometimes be written as $\{x_{1:T}, b_{1:T-1}, j, u_{1:T}^{(-j)}\}$ without ambiguity.

We now assume Assumptions S1 and S2, given in Section S1 of the online supplement. The target distribution from Andrieu et al. [2010] is

$$\tilde{\pi}^N \left(x_{1:T}, b_{1:T-1}, j, u_{1:T}^{(-j)}, \theta \right) := \frac{p(x_{1:T}, \theta | y_{1:T})}{N^T} \frac{\psi(u_{1:T} | \theta)}{m_1^\theta(x_1^{b_1}) \prod_{t=2}^T \bar{w}_{t-1}^{a_t^{b_t}} m_t^\theta \left(x_t^{b_t} | x_{t-1}^{a_{t-1}^{b_t}} \right)}, \quad (3)$$

where $u_{1:T}$ is given in Eq. (1). Assumption S1 ensures that $\tilde{\pi}^N(u_{1:T} | \theta)$ is absolutely continuous with respect to $\psi(u_{1:T} | \theta)$, so that $\psi(u_{1:T} | \theta)$ can be used as a Metropolis-Hastings proposal density for generating from $\tilde{\pi}^N(u_{1:T} | \theta)$.

From Assumption S2, Eq. (3) has the following marginal distribution

$$\tilde{\pi}^N(x_{1:T}, b_{1:T-1}, j, \theta) = \frac{p(x_{1:T}, \theta | y_{1:T})}{N^T}, \quad (4)$$

and hence $\tilde{\pi}^N(x_{1:T}, \theta) = p(x_{1:T}, \theta | y_{1:T})$. The online supplement gives further details.

2.3 Conditional sequential Monte Carlo (CSMC)

The particle Gibbs algorithm in Andrieu et al. [2010] uses exact conditional distributions to construct a Gibbs sampler. If we use the *ancestral tracing* augmented distribution given in (3), then this includes the conditional distribution given by $\tilde{\pi}^N(u_{1:T}^{(-j)} | x_{1:T}^j, b_{1:T-1}^j, j, \theta)$, which involves constructing the particle approximation conditional on a pre-specified path. The *conditional sequential Monte Carlo* algorithm, introduced in Andrieu et al. [2010], is a sequential Monte Carlo algorithm in which a particle $X_{1:T}^J = (X_1^{B_1^J}, \dots, X_T^{B_T^J})$, and the associated sequence of ancestral indices $B_{1:T-1}^J$ are kept unchanged. In other words, the conditional sequential Monte Carlo algorithm is a procedure that resamples all the particles and indices except for $U_{1:T}^J = (X_{1:T}^J, A_{1:T-1}^J) = (X_1^{B_1^J}, \dots, X_T^{B_T^J}, B_1^J, \dots, B_{T-1}^J)$. Algorithm S2 of the supplementary material describes the conditional sequential Monte Carlo algorithm (as in Andrieu et al. [2010]), consistent with $(x_{1:T}^j, a_{1:T-1}^j, j)$.

2.4 Flexible sampling scheme for state space models

This section introduces a sampling scheme that is suitable for the state space form given in Section 2.1, where some of the parameters can be generated exactly conditional on the state vectors using PG step, but other parameters must be generated using PMMH step. For simplicity, let $\theta := (\theta_1, \theta_2)$ be a partition of the parameter vector into 2 components where each component may be a vector. Let $\Theta = \Theta_1 \times \Theta_2$ be the corresponding partition of the parameter space. The following sampling scheme generates the vector of parameter θ_1 using PMMH step and the vector of parameter θ_2 using PG step. We call this a PMMH+PG sampler. It is important to note that the components in the parameter vector θ_1 can be sampled separately in multiple PMMH steps and the components in the parameter vector θ_2 can be sampled separately in multiple Gibbs steps. Details are given in Section S2 in the online supplement.

Sampling Scheme 1 (PMMH+PG Sampler) *Given initial values for $U_{1:T}$, J and θ , one iteration of the MCMC involves the following steps.*

1. (PMMH sampling)

- (a) Sample $\theta_1^* \sim q_{1,1}(\cdot | U_{1:T}, J, \theta_2, \theta_1)$.
- (b) Sample $U_{1:T}^* \sim \psi(\cdot | \theta_2, \theta_1^*)$.
- (c) Sample $J^* \sim \tilde{\pi}^N(\cdot | U_{1:T}^*, \theta_2, \theta_1^*)$.
- (d) Set $(\theta_1, U_{1:T}, J) \leftarrow (\theta_1^*, U_{1:T}^*, J^*)$ with probability

$$\alpha_1(U_{1:T}, J, \theta_1; U_{1:T}^*, J^*, \theta_1^* | \theta_2) = 1 \wedge \frac{\tilde{\pi}^N(U_{1:T}^*, \theta_1^* | \theta_2)}{\tilde{\pi}^N(U_{1:T}, \theta_1 | \theta_2)} \frac{q_1(U_{1:T}, \theta_1 | U_{1:T}^*, J^*, \theta_2, \theta_1^*)}{q_1(U_{1:T}^*, \theta_1^* | U_{1:T}, J, \theta_2, \theta_1)}, \quad (5)$$

where

$$q_1(U_{1:T}^*, \theta_1^* | U_{1:T}, J, \theta_2, \theta_1) = q_{1,1}(\theta_1^* | U_{1:T}, J, \theta_2, \theta_1) \psi(U_{1:T}^* | \theta_2, \theta_1^*).$$

2. (PG sampling)

- (a) Sample $\theta_2^* \sim q_2(\cdot | X_{1:T}^J, B_{1:T-1}^J, J, \theta_2, \theta_1)$.
- (b) Set $\theta_2 \leftarrow \theta_2^*$ with probability

$$\alpha_2(\theta_2; \theta_2^* | X_{1:T}^J, B_{1:T-1}^J, J, \theta_1) = 1 \wedge \frac{\tilde{\pi}^N(\theta_2^* | X_{1:T}^J, B_{1:T-1}^J, J, \theta_1)}{\tilde{\pi}^N(\theta_2 | X_{1:T}^J, B_{1:T-1}^J, J, \theta_1)} \times \frac{q_2(\theta_2 | X_{1:T}^J, B_{1:T-1}^J, J, \theta_1, \theta_2^*)}{q_2(\theta_2^* | X_{1:T}^J, B_{1:T-1}^J, J, \theta_1, \theta_2)}. \quad (6)$$

- 3. Sample $U_{1:T}^{(-J)} \sim \tilde{\pi}^N(\cdot | X_{1:T}^J, B_{1:T-1}^J, J, \theta)$ using the conditional sequential Monte Carlo algorithm (CSMC) discussed in Section 2.3.

4. Sample $J \sim \tilde{\pi}^N(\cdot|U_{1:T}, \theta)$.

The generalization of the sampling scheme to the case where the components in the parameter vector θ_1 are sampled separately in multiple PMMH steps and the components in the parameter vector θ_2 are sampled separately in multiple Gibbs steps is straightforward and involves repeated steps of the same form as given in Part 1 and Part 2 respectively.

Note that Parts 2 to 4 are the same as the particle Gibbs sampler described in Andrieu et al. [2010] or the particle Metropolis within Gibbs sampler described in Lindsten and Schön [2012a]. Part 1 differs from the particle Marginal Metropolis-Hastings approach discussed in Andrieu et al. [2010] by generating the variable J which selects the trajectory. This is necessary since J is used in Part 2.

A major computational cost of the algorithm is generating the particles p^* times in Part 1, where p^* is the number of PMMH steps, as well as running the CSMC algorithm in Part 3. Hence there is a computational cost in using the PMMH+PG sampler compared to a particle Gibbs sampler. Similar comments apply to a blocked PMMH sampler.

Section S2 of the supplementary material discusses the convergence of Sampling Scheme 1 to its target distribution.

Remark 1 *Andrieu et al. [2010] show that*

$$\frac{\tilde{\pi}^N(U_{1:T}, \theta_1 | \theta_2)}{\psi(U_{1:T} | \theta_2, \theta_1)} = \frac{Z(U_{1:T}, \theta) p(\theta_1 | \theta_2)}{p(y_{1:T} | \theta_2)}, \quad (7)$$

and hence the Metropolis-Hastings acceptance probability in Eq. (S1) simplifies to

$$1 \wedge \frac{Z(\theta_1^*, \theta_2, U_{1:T}^*)}{Z(\theta_1, \theta_2, U_{1:T})} \frac{q_{1,1}(\theta_1 | U_{1:T}^*, J^*, \theta_2, \theta_1^*) p(\theta_1^* | \theta_2)}{q_{1,1}(\theta_1^* | U_{1:T}, J, \theta_2, \theta_1) p(\theta_1 | \theta_2)}. \quad (8)$$

Equation (8) shows the PMMH steps can be viewed as involving a particle approximation to an ideal sampler which we use to estimate the likelihood of the model. This version of the PMMH algorithm can also be viewed as a Metropolis-Hastings algorithm using an unbiased estimate of the likelihood.

Remark 2 *Part 1 of the sampling scheme is a good choice for parameter vector θ_1 which is highly correlated with the state vector $X_{1:T}$. Part 2 of the sampling scheme is a good choice if the parameter vector θ_2 is not highly correlated with the states and it is possible to sample exactly from the distribution $\tilde{\pi}^N(\theta_2 | X_{1:T}^J, B_{1:T-1}^J, J, \theta_1)$ or a good approximation is available as a Metropolis-Hastings proposal. Using Eq. (4), the Metropolis-Hastings acceptance probability in Eq. (S2) simplifies to*

$$\frac{p(y_{1:T} | X_{1:T}^J, \theta_2^*, \theta_1) p(X_{1:T}^J | \theta_2^*, \theta_1) p(\theta_2^* | \theta_1)}{p(y_{1:T} | X_{1:T}^J, \theta_2, \theta_1) p(X_{1:T}^J | \theta_2, \theta_1) p(\theta_2 | \theta_1)} \times \frac{q_2(\theta_2 | X_{1:T}^J, B_{1:T-1}^J, J, \theta_1, \theta_2^*)}{q_2(\theta_2^* | X_{1:T}^J, B_{1:T-1}^J, J, \theta_1, \theta_2)}. \quad (9)$$

See Lindsten and Schön [2012a] for more discussion about the particle Metropolis-Hastings within Gibbs proposals in Part 2.

3 Univariate Example: The univariate continuous time Ornstein-Uhlenbeck process

This section applies the PMMH + PG sampler defined in Section 2.4 to the univariate continuous time Ornstein-Uhlenbeck SV model with covariates in the mean.

3.1 Definition of inefficiency

To define our measure of the inefficiency of a sampler that takes computing time into account, we first define the integrated autocorrelation time (IACT) for a univariate parameter θ ,

$$\text{IACT}_\theta := 1 + 2 \sum_{j=1}^{\infty} \rho_{j,\theta} \quad (10)$$

where $\rho_{j,\theta}$ is the correlation of the iterates of θ in the MCMC after the chain has converged. A large value of IACT for one or more of the parameters indicates that the chain does not mix well.

We estimate IACT_θ based on M iterates $\theta^{[1]}, \dots, \theta^{[M]}$ (after convergence) as

$$\widehat{\text{IACT}}_{\theta,M} = 1 + 2 \sum_{j=1}^{L_M} \widehat{\rho}_{j,\theta},$$

where $\widehat{\rho}_{j,\theta}$ is the estimate of $\rho_{j,\theta}$, $L_M = \min(1000, L)$ and $L = \min_{j \leq M} |\widehat{\rho}_{j,\theta}| < 2/\sqrt{M}$ because $1/\sqrt{M}$ is approximately the standard error of the autocorrelation estimates when the series is white noise. Let $\widehat{\text{IACT}}_{\text{MAX}}$ and $\widehat{\text{IACT}}_{\text{MEAN}}$ be the maximum and mean of the estimated IACT values over all the parameters in the model, respectively. Our measure of the inefficiency of a sampler based on $\widehat{\text{IACT}}_{\text{MAX}}$ is the time normalized variance (TNV),

$$\text{TNV}_{\text{MAX}} = \widehat{\text{IACT}}_{\text{MAX}} \times \text{CT}, \quad (11)$$

where CT is the computing time in seconds per iteration; we define the inefficiency of a sampler based on $\widehat{\text{IACT}}_{\text{MEAN}}$ similarly. The relative time normalized variance (RTNV) shows the TNV relative to our method.

3.2 The univariate continuous time Ornstein-Uhlenbeck process

We consider the model

$$y_t = z_t' \beta + \exp(h_t/2) \varepsilon_t, \quad \text{where } \varepsilon_t \sim N(0, 1), \quad (12)$$

with the log-volatility h_t generated by the continuous time Ornstein-Uhlenbeck (OU) process $\{h_t\}_{t \geq 1}$, introduced by Stein and Stein [1991]. This process satisfies,

$$dh_t = \alpha(\mu - h_t) dt + \tau dW_t, \quad (13)$$

where W_t is a Wiener process. The transition densities for h_t have the closed form [Brix et al., 2018, p. 7]

$$h_t|h_{t-1} \sim N\left(\mu + \exp(-\alpha)(h_{t-1} - \mu), \frac{1 - \exp(-2\alpha)}{2\alpha}\tau^2\right), \quad (14)$$

with $h_1 \sim N\left(\mu, \frac{\tau^2}{2\alpha}\right)$. This is a state space model of the form given in Section 2.1 with $x_{1:T} = h_{1:T}$ and whose parameters are $\alpha > 0$, $\mu, \tau^2 > 0$, and $(m_\beta \times 1)$ vector β . This is a general time series model that allows for a scalar dependent variable y_t with possible dependence on covariates in the mean as well as stochastic variance terms. Thus, $E(y_t|z_t, h_t, \theta) = z_t'\beta$, where z_t can consist of lags of y_t ; $\text{Var}(y_t|z_t, h_t, \theta) = \exp(h_t)$. The model can be applied to many time series and has been extensively used in the financial econometrics literature. It is straightforward to generalise this model in a number of ways: for example, by allowing for covariates in the conditional variance and including conditional variance term in the mean. See Durbin and Koopman [2012, pp. 216-221], who discuss the basic stochastic volatility model and some extensions.

Many stochastic volatility diffusion models do not have a closed form transition density, e.g., the continuous time GARCH diffusion process Chib et al. [2004], Kleppe et al. [2010] discussed in Section 4.1, and it is then necessary to estimate such state space models using an approximation such as the Euler discretization. It is therefore informative to study the relative performance of the PG+PMMH sampler for the OU process using both the closed form transition equation in Eq. (19) as well as the OU with the Euler approximation in Eq. (15), to see the relative loss due to the approximation.

The Euler scheme approximates the evolution of the log-volatilities h_t in equation (13) by placing $M - 1$ evenly spaced points between times t and $t + 1$. We denote the intermediate volatility components by $h_{t,1}, \dots, h_{t,M-1}$, and it is convenient to set $h_{t,0} = h_t$ and $h_{t,M} = h_{t+1}$. The equation for the Euler evolution, starting at $h_{t,0}$ is (see, for example, Stramer and Bognar [2011], pg. 234)

$$h_{t,j}|h_{t,j-1} \sim N\left(h_{t,j-1} + \alpha(\mu - h_{t,j-1})\delta, \tau^2\delta\right), \quad (15)$$

for $j = 1, \dots, M$, where $\delta = 1/M$.

3.3 Empirical results

We use the following notation to describe the algorithm used in this example. The basic samplers, as used in Sampling Scheme 1, are PMMH(\cdot) and PG(\cdot). These samplers can be used alone or in combination. For example, PMMH(θ) means using a PMMH step to sample the parameter vector θ ; PMMH(θ_1) + PG(θ_2) means sampling θ_1 in the PMMH step and θ_2 in the PG step; and PG(θ) means sampling θ using the PG sampler. Our general procedure to determine an efficient sampling scheme is to first run a PG algorithm to identify which parameters have large IACT, or, in some cases, require a large amount of computational time to generate in the PG step. We then generate these parameters in the PMMH step.

Univariate OU model with exact transition density and no covariate

In this section, we consider the univariate OU model with exact transition density and no covariate ($m_\beta = 0$). We compare the performance of the following samplers: (I) PMMH (α, τ^2) + PG (μ), (II) the particle Gibbs with ancestral tracing approach of Andrieu et al. [2010] (PGAT (μ, τ^2, α)), (III) the particle Gibbs with backward simulation approach of Lindsten and Schon [2013] (PGBS (μ, τ^2, α)), (IV) PMMH with an adaptive random walk as the proposal density for the parameters (PMMH-RW (μ, τ^2, α)), (V) PMMH with the Metropolis adjusted Langevin algorithm (MALA) of Nemeth et al. [2016b] for the proposal for the parameters (PMMH-MALA (μ, τ^2, α)), (VI) the correlated PMMH approach of Deligiannidis et al. [2018] with an adaptive random walk as the proposal density for the parameters (Corr. PMMH-RW (μ, τ^2, α)), (VII) the correlated PMMH approach of Deligiannidis et al. [2018] with the Metropolis adjusted Langevin algorithm of Nemeth et al. [2016b] as the proposal for the parameters (Corr. PMMH-MALA (μ, τ^2, α)), and (VIII) the particle Gibbs with data augmentation approach of Fearnhead and Meligkotsidou [2016] (PGDA (μ, τ^2, α)). The score vector required for the MALA algorithm is estimated efficiently using methods described in Nemeth et al. [2016a]. The tuning parameters of the PGDA sampler are set optimally according to the approach described in Fearnhead and Meligkotsidou [2016]. The correlated PMMH proposed by Deligiannidis et al. [2018] correlates the random vectors \mathbf{u} and \mathbf{u}' used to construct the estimators of the likelihood at the current and proposed values of the parameters (θ and θ' respectively). This is done to reduce the variance of the difference between $\log \left(Z_{1:T}(\theta', \mathbf{u}') \right) - \log \left(Z_{1:T}(\theta, \mathbf{u}) \right)$ which appears in the PMMH acceptance ratio. The correlated PMMH significantly reduces the number of particles required by the standard pseudo marginal method proposed by Andrieu et al. [2010]. We use $N = 500$ particles for the PMMH+PG, PGAT, PGBS, PMMH and PGDA samplers, and $N = 50$ for the correlated PMMH sampler. In this example, we use the bootstrap particle filter to sample the particles for all samplers and the adaptive random walk in Roberts and Rosenthal [2009] for the PMMH step in the PMMH+PG sampler as the proposal density for the parameters. The particle filter and the parameter samplers are implemented in Matlab.

We apply the methods to a sample of daily US steel industry stock returns data obtained from the Kenneth French website¹, using a sample from January 3rd, 2001 to the 24th of December, 2003, a total of 1,000 observations. The priors for the OU parameters are $\alpha \sim IG\left(\frac{v_0}{2}, \frac{s_0}{2}\right)$, $\tau^2 \sim IG\left(\frac{v_0}{2}, \frac{s_0}{2}\right)$, where $v_0 = 10$ and $s_0 = 1$, $p(\mu) \propto 1$, and $p(\beta) \propto 1$. These prior densities cover most possible values in practice. We ran all the sampling schemes for 11,000 iterations and discarded the initial 1,000 iterations as warmup for all the methods.

Table 1 shows the IACT, TNV, and RTNV values for the parameters in the univariate OU model with an exact transition density and no covariate estimated using the 8 different samplers described above. The table shows the following points. (1) Both the PGAT and PGBS samplers have large IACT values for both parameters α and τ^2 , and we show that putting those two parameters in the PMMH step improves the mixing significantly. We show later in this section and in Section 4.2 that it is also beneficial to use a PMMH step for at least the

¹<http://mba.tuck.dartmouth.edu/pages/faculty/ken.french/datalibrary.html>

α and τ^2 parameters for the stochastic volatility diffusion models that use an approximation such as the Euler discretization. (2) In terms of $\widehat{\text{TNV}}_{\text{MEAN}}$, the PMMH+PG sampler is 3.18, 3.12, 1.08, and 1.51 times better than the PGAT, PGBS, Corr. PMMH-MALA, and PGDA samplers respectively, and the PMMH-RW, PMMH-MALA, and correlated PMMH-RW methods are 1.33, 2.56, and 1.88 times better than the PMMH+PG sampler, respectively. Similar conclusions can be made based on $\widehat{\text{TNV}}_{\text{MAX}}$. (3) The best sampler for this example is the correlated PMMH-RW. (4) The PMMH-MALA sampler has lower IACT values for all the parameters compared to the PMMH-RW sampler, but the correlated PMMH-RW sampler is better than the correlated PMMH-MALA sampler. This shows that there is no advantage of using particle MALA over the random walk proposal. It is therefore important to note that although the correlated PMMH can significantly reduce the number of particles required compared to standard PMMH, the variance of the estimate of the gradient of the log-posterior is not sufficiently small with the choice of $N = 50$ particles used by the correlated PMMH sampler. This confirms the observation made by Nemeth et al. [2016b] who write “Our results show that the behaviour of particle MALA depends on how accurately we can estimate the gradient of the log-posterior. If the error in the estimate of the gradient is not controlled sufficiently well as we increase dimension, then asymptotically there will be no advantage in using particle MALA over a particle MCMC algorithm using a random-walk proposal”. (5) The PGDA sampler has lower IACT values for both α and τ^2 parameters compared to the PGBS and PGAT samplers, but it has higher IACT value for μ . This shows that the PGDA sampler is useful to improve the mixing of the parameters that are highly correlated with the states.

Table 1: Inefficiency factors of α , τ^2 , and μ for the Univariate OU model with an exact transition density and without covariates for the US steel industry stock returns data with $T = 1000$. Sampler I: PMMH(α, τ^2) + PG(μ), Sampler II: PGAT(μ, τ^2, α), Sampler III: PGBS(μ, τ^2, α), Sampler IV: PMMH-RW(μ, τ^2, α), Sampler V: PMMH-MALA(μ, τ^2, α), Sampler VI: Correlated PMMH-RW(μ, τ^2, α), Sampler VII: Correlated PMMH-MALA(μ, τ^2, α), and Sampler VIII: PGDA(μ, τ^2, α).

Param	I	II	III	IV	V	VI	VII	VIII
α	12.01	50.21	40.12	15.02	4.62	13.00	12.38	18.06
μ	1.56	1.65	1.48	12.81	4.59	14.17	28.77	9.16
τ^2	13.49	85.46	70.98	12.64	4.74	11.18	17.20	19.42
$\widehat{\text{IACT}}_{\text{MAX}}$	13.49	85.46	70.98	15.02	4.74	14.17	28.77	19.42
$\widehat{\text{TNV}}_{\text{MAX}}$	2.16	8.55	8.52	1.20	0.57	0.85	2.30	2.72
$\widehat{\text{RTNV}}_{\text{MAX}}$	1	3.95	3.94	0.56	0.26	0.39	1.06	1.25
$\widehat{\text{IACT}}_{\text{MEAN}}$	9.02	45.77	37.53	13.49	4.65	12.78	19.45	15.55
$\widehat{\text{TNV}}_{\text{MEAN}}$	1.44	4.58	4.50	1.08	0.56	0.77	1.56	2.17
$\widehat{\text{RTNV}}_{\text{MEAN}}$	1	3.18	3.12	0.75	0.39	0.53	1.08	1.51
Time	0.16	0.10	0.12	0.08	0.12	0.05	0.08	0.14

Univariate OU model with exact transition density and 50 covariates

We now consider the univariate OU model with an exact transition density and $m_\beta = 50$ covariates. We compare the performance of the following samplers: (1) PMMH(α, τ^2) + PG(μ, β), (2) PGAT($\mu, \tau^2, \alpha, \beta$), (3) PGBS($\mu, \tau^2, \alpha, \beta$), (4) PMMH-RW($\mu, \tau^2, \alpha, \beta$), (5) PMMH-MALA($\mu, \tau^2, \alpha, \beta$), (6) Corr. PMMH-RW($\mu, \tau^2, \alpha, \beta$), (7) Corr. PMMH-MALA($\mu, \tau^2, \alpha, \beta$), and (8) PGDA($\mu, \tau^2, \alpha, \beta$). We use $N = 500$ particles for the PMMH+PG, PGAT, PGBS, PMMH, and PGDA samplers, and $N = 50$ for the correlated PMMH sampler. We simulated data with $T = 1000$ and set $\alpha = 0.09$, $\mu = 0.38$, $\tau^2 = 0.08$, and $\beta_i = 0.1$ for $i = 1, \dots, m_\beta$. The covariates are $z_t \sim N(0, I_{50})$.

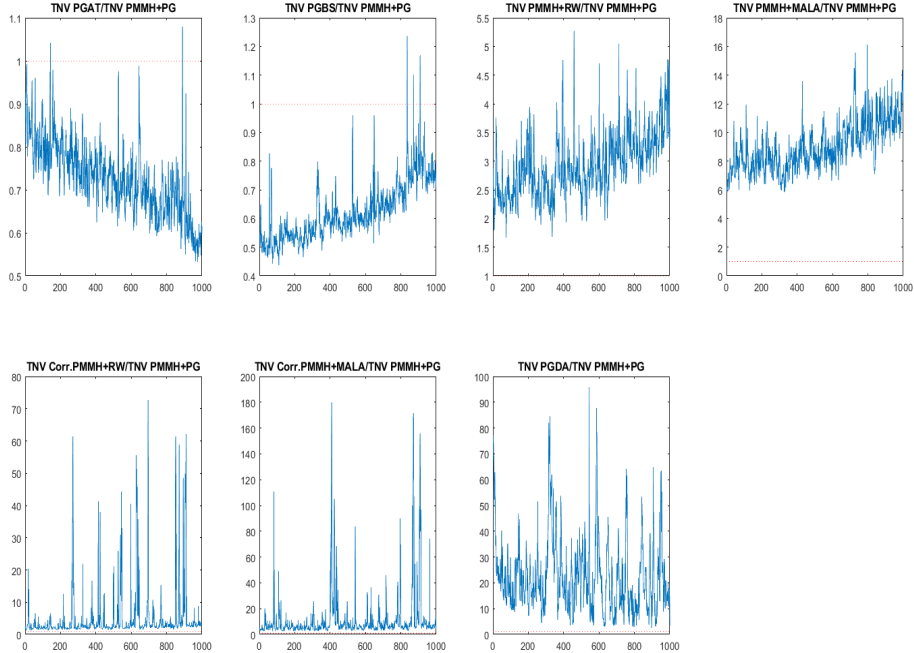
Table 2 shows the IACT, TNV, and RTNV values for the parameters in the univariate OU model with an exact transition density and 50 covariates estimated using the 8 different samplers listed above. The table shows the following points. (1) The best sampler for this example is the PMMH+PG sampler. This example shows how the PMMH and PG samplers can be combined in a flexible manner to obtain good results. In this example, the vector of parameters β are high dimensional and not highly correlated with the states, so it is important to generate them in a PG step. Both α and τ^2 are generated in a PMMH step because they are highly correlated with the states. (2) The standard and correlated PMMH with adaptive random walks are much worse than the PMMH+PG sampler because the adaptive random walk proposal is inefficient in high dimensions. (3) The correlated PMMH with the MALA proposal is worse than the correlated PMMH with an adaptive random walk proposal and is the worst sampler in this example because the variance of the gradient of log-posterior is not sufficiently small with the number of particles set to $N = 50$. (4) The PGDA sampler has very large IACT values for all parameters indicating that the PGDA sampler does not perform well for models with a large number of parameters.

Figure 1 shows the RTNV of the PMMH+PG sampler over other samplers for the log-volatilities $h_{1:T}$ for all t . The figure shows that the PMMH+PG sampler is much more efficient than the standard and correlated PMMH samplers and the PGDA sampler. It is only slightly worse than the PGAT and PGBS samplers.

Table 2: Inefficiency factors of α , τ^2 , and μ for the Univariate OU model with an exact transition density and $m_\beta = 50$ covariates for the simulated data with $T = 1000$. Sampler I: PMMH (α, τ^2) + PG (β, μ), Sampler II: PGAT ($\beta, \mu, \tau^2, \alpha$), Sampler III: PGBS ($\beta, \mu, \tau^2, \alpha$), Sampler IV: PMMH-RW ($\beta, \mu, \tau^2, \alpha$), Sampler V: PMMH-MALA ($\beta, \mu, \tau^2, \alpha$), Sampler VI: Correlated PMMH-RW ($\beta, \mu, \tau^2, \alpha$), Sampler VII: Correlated PMMH-MALA ($\beta, \mu, \tau^2, \alpha$), and Sampler VIII: PGDA ($\beta, \mu, \tau^2, \alpha$).

Param	I	II	III	IV	V	VI	VII	VIII
α	11.15	47.14	40.94	281.68	33.15	135.17	561.44	356.24
μ	1.58	1.73	1.81	377.59	17.79	84.31	931.89	211.48
τ^2	14.50	95.55	71.83	341.19	20.43	81.17	1368.65	296.52
mean (β)	1.52	1.57	1.46	165.50	14.43	131.88	958.51	276.13
max (β)	1.80	1.95	1.71	545.26	21.76	434.50	1445.25	690.57
$\widehat{\text{IACT}}_{\text{MAX}}$	14.50	95.55	71.83	545.26	33.15	434.50	1445.25	690.57
$\widehat{\text{TNV}}_{\text{MAX}}$	2.47	9.55	9.34	43.62	7.96	26.07	130.07	227.89
$\widehat{\text{RTNV}}_{\text{MAX}}$	1	3.87	3.78	17.66	3.22	10.55	52.66	92.26
$\widehat{\text{IACT}}_{\text{MEAN}}$	1.95	4.21	3.53	175.00	14.96	130.10	958.26	276.81
$\widehat{\text{TNV}}_{\text{MEAN}}$	0.33	0.42	0.46	14.00	3.59	7.81	86.24	91.35
$\widehat{\text{RTNV}}_{\text{MEAN}}$	1	1.27	1.39	42.42	10.88	23.67	261.33	276.82
Time	0.17	0.10	0.13	0.08	0.24	0.06	0.09	0.33

Figure 1: The Inefficiency Factors for the log-volatilities $h_{1:T}$ for the univariate OU model with 50 covariates for simulated data with $T = 1000$. The relative Time Normalised Variance (RTNV) is computed relative to the PMMH+PG sampler



Univariate OU model with Euler approximation for the state transition density and 50 covariates

Lastly, we consider the univariate OU model with an Euler approximation for the state transition density and $m_\beta = 50$ covariates. We compare the performance of the following samplers: (1) PMMH (μ, α, τ^2) + PG (β), (2) PGAT ($\mu, \tau^2, \alpha, \beta$), (3) PGBS ($\mu, \tau^2, \alpha, \beta$). We used $N = 500$ particles for all samplers and $M = 10$ latent points for the Euler approximation of the state transition density.

Table 3 shows the IACT, TNV, and RTNV values for the parameters in the univariate OU model with an Euler approximation for the state transition density and 50 covariates. The table shows the following points. (1) The PMMH+PG samplers with exact and approximate state transition densities have very similar IACT values suggesting that the inefficiency of the PMMH+PG sampler does not deteriorate when the Euler approximation is used. However, both the PGAT and PGBS samplers using the Euler approximation are significantly worse than the PGAT and PGBS samplers with exact transition densities. (2) The best sampler is the PMMH+PG sampler. (3) It is interesting to see that when we use an Euler approximation for the diffusion the PMMH+PG, PGAT, and PGBT samplers all take approximately the same computing time. This is because the PGAT and PGBT samplers need to store and

trace back all the latent log-volatilities h_t and the M latent data points between t and $t + 1$ for all $t = 1, \dots, T$, whereas the PMMH+PG sampler only needs to store and trace back the latent log-volatilities h_t for all $t = 1, \dots, T$. Therefore, the PMMH+PG sampler is also more efficient in terms of memory usage if it is necessary to use an Euler approximation.

In summary, in this univariate example, we show the following points. (1) The inefficiency of the PMMH+PG sampler does not deteriorate when the Euler approximation is used, whereas both the PGAS and PGAT samplers are significantly worse. (2) PGDA is useful to improve the mixing of the parameters that are highly correlated with the states, but it does not work for models with many parameters. (3) The PMMH+PG sampler is much more efficient than the standard and correlated PMMH samplers with adaptive random walk proposals because the random walk proposals are inefficient in high dimensions. (4) There is no advantage of using particle MALA over the random walk proposal when the variance of the estimate of the gradient of the log-posterior is not sufficiently small. (5) It is desirable to generate parameters that are highly correlated with the states using a PMMH step that does not condition on the states. Conversely, if there is a subset of parameters that is not highly correlated with the states, then it is preferable to generate them using a particle Gibbs step, or a particle Metropolis within Gibbs step, that conditions on the states, especially when the subset is large. In general, using PG may be preferred to PMMH whenever possible, because it may be easier to obtain better proposals within a PG framework. (6) Our PMMH + PG approach can be further refined by using the data augmented PMMH and PG sampling schemes proposed by Fearnhead and Meligkotsidou [2016] and the refined proposals for the PMMH sampling scheme by Dahlin et al. [2015] and Nemeth et al. [2016b].

Table 3: Univariate OU model with $m_\beta = 50$ covariates and Euler approximation for the state transition density for the simulated data with $T = 1000$. Sampler I: PMMH (α, τ^2, μ) + PG (β), Sampler II: PGAT ($\beta, \mu, \tau^2, \alpha$), Sampler III: PGBS ($\beta, \mu, \tau^2, \alpha$).

Param	I	II	III
α	12.23	175.33	130.71
μ	13.56	18.09	15.22
τ^2	10.99	403.72	347.64
mean (β)	1.52	1.55	1.46
max (β)	1.72	1.87	1.72
$\widehat{\text{IACT}}_{\text{MAX}}$	13.56	403.72	347.64
$\widehat{\text{TNV}}_{\text{MAX}}$	3.53	117.08	111.24
$\widehat{\text{RTNV}}_{\text{MAX}}$	1	33.17	31.51
$\widehat{\text{IACT}}_{\text{MEAN}}$	2.13	12.73	10.69
$\widehat{\text{TNV}}_{\text{MEAN}}$	0.55	3.69	3.42
$\widehat{\text{RTNV}}_{\text{MEAN}}$	1	6.71	6.22
Time	0.26	0.29	0.32

4 Multivariate Example

This section applies the ideas in this paper to the multivariate factor stochastic volatility model, which is a serious complex example. It also shows how a complex particle MCMC scheme can be built from the basic PMMH + PG sampler in Section 2.4. Section 4.1 discusses the multivariate factor stochastic volatility model. Section 4.2 compares the performance of the PMMH+PG sampler to other competing PMCMC methods to estimate multivariate factor SV models using both simulated and real datasets.

4.1 The factor stochastic volatility model

Factor stochastic volatility (SV) models are a popular approach to jointly model many co-varying financial time series, as they are able to capture their common features using only a small number of latent factors (see, e.g., Chib et al. [2006] and Kastner et al. [2017]). However, estimating time-varying multivariate factor SV models can be very challenging because the likelihood involves calculating an integral over a very high-dimensional latent state space, and the number of parameters in the model can be large.

We consider a factor SV model with the volatilities of the factors following a traditional SV model [Chib et al., 2006, Kastner et al., 2017], while the log volatilities of the idiosyncratic errors follow continuous time Ornstein-Uhlenbeck (OU) processes [Stein and Stein, 1991] or GARCH diffusion processes [Chib et al., 2004, Kleppe et al., 2010]. The log volatility of an OU process admits a closed form state transition density, see Section 3.2, whereas the GARCH diffusion process does not. Our estimation methods are applied to Euler approximations of the diffusion process driving the log volatilities, and hence can handle diffusions that do not admit closed form transition densities; see Ignatieva et al. [2015] for other diffusions whose transition equations need an Euler approximation because they cannot be expressed in closed form. It is informative to study the closed form and Euler approximation for the state transition density for the OU process in the multivariate case to see the relative loss due to the approximation.

Suppose that \mathbf{P}_t is a $S \times 1$ vector of daily stock prices and define $\mathbf{y}_t := \log \mathbf{P}_t - \log \mathbf{P}_{t-1}$ as the log-return of the stocks. We model \mathbf{y}_t as the factor SV model

$$\mathbf{y}_t = \boldsymbol{\beta} \mathbf{f}_t + \mathbf{V}_t^{\frac{1}{2}} \boldsymbol{\epsilon}_t \quad (t = 1, \dots, T), \quad (16)$$

where \mathbf{f}_t is a $K \times 1$ vector of latent factors (with $K \ll S$), $\boldsymbol{\beta}$ is a $S \times K$ factor loading matrix of unknown parameters. Appendix S5.2 gives further details on the restrictions on $\boldsymbol{\beta}$. We model the latent factors as $\mathbf{f}_t \sim N(0, \mathbf{D}_t)$ and $\boldsymbol{\epsilon}_t \sim N(0, I)$, so that $\mathbf{y}_t | (\mathbf{f}_t, \mathbf{h}_t) \sim N(\boldsymbol{\beta} \mathbf{f}_t, \mathbf{V}_t)$. The time-varying variance matrices \mathbf{D}_t and \mathbf{V}_t depend on unobserved random variables $\boldsymbol{\lambda}_t = (\lambda_{1,t}, \dots, \lambda_{K,t})$ and $\mathbf{h}_t = (h_{1,t}, \dots, h_{S,t})$ such that

$$\mathbf{D}_t := \text{diag}(\exp(\lambda_{1,t}), \dots, \exp(\lambda_{K,t})), \quad \mathbf{V}_t := \text{diag}(\exp(h_{1,t}), \dots, \exp(h_{S,t})).$$

Each $\lambda_{k,t}$ is assumed to follow an independent autoregressive process

$$\lambda_{k,t} = \phi_k \lambda_{k,t-1} + \tau_{f,k} \eta_{k,t}, \quad k = 1, \dots, K, \quad (17)$$

with $\eta_{k,t} \sim N(0, 1)$. The log volatilities $h_{s,t}$ follow either a Gaussian OU continuous time volatility process or a GARCH diffusion continuous time volatility process.

The continuous time Ornstein-Uhlenbeck (OU) process $\{h_{s,t}\}_{t \geq 1}$ discussed in Section 3.2 satisfies

$$dh_{s,t} = \alpha_s (\mu_s - h_{s,t}) dt + \tau_{\epsilon,s} dW_{s,t}, \quad \text{for } s = 1, \dots, S, \quad (18)$$

where $W_{s,t}$ is a Wiener process. The transition distribution for each $h_{s,t}$ is [Brix et al., 2018, p. 7]

$$h_{s,t}|h_{s,t-1} \sim N\left(\mu_s + \exp(-\alpha_s)(h_{s,t-1} - \mu_s), \frac{1 - \exp(-2\alpha_s)}{2\alpha_s} \tau_{\epsilon,s}^2\right), \quad s = 1, \dots, S. \quad (19)$$

with $h_{s,1} \sim N\left(\mu_s, \frac{\tau_{\epsilon,s}^2}{2\alpha_s}\right)$. The parameters are $\alpha_s > 0$, μ_s and $\tau_{\epsilon,s}^2 > 0$.

The Euler scheme approximates the evolution of the log-volatilities $h_{s,t}$ in equation (18). We use the approach in Section 3.2 by placing $M - 1$ evenly spaced points between times t and $t + 1$. The intermediate volatility components are denoted by $h_{s,t,1}, \dots, h_{s,t,M-1}$, and it is convenient to set $h_{s,t,0} = h_{s,t}$ and $h_{s,t,M} = h_{s,t+1}$. The equation for the Euler evolution, starting at $h_{s,t,0}$ is (see, for example, Stramer and Boggar [2011], pg. 234)

$$h_{s,t,j}|h_{s,t,j-1} \sim N\left(h_{s,t,j-1} + \alpha_s (\mu_s - h_{s,t,j-1}) \delta, \tau_{\epsilon,s}^2 \delta\right), \quad (20)$$

for $j = 1, \dots, M$, where $\delta = 1/M$.

The continuous time GARCH diffusion process $\{h_{s,t}\}_{t \geq 1}$ [Chib et al., 2004, Kleppe et al., 2010] satisfies

$$dh_{s,t} = \left\{ \alpha_s (\mu_s - \exp(h_{s,t})) \exp(-h_{s,t}) - \frac{\tau_{\epsilon,s}^2}{2} \right\} dt + \tau_{\epsilon,s} dW_{s,t}, \quad \text{for } s = 1, \dots, S, \quad (21)$$

where the $W_{s,t}$ are independent Wiener processes. The Euler approximation of the state transition density of equation (21) yields the transition density between steps (see for example, Wu et al. [2018], pg. 21)

$$h_{s,t,j+1}|h_{s,t,j} \sim N\left(h_{s,t,j} + \left\{ \alpha_s (\mu_s - \exp(h_{s,t,j})) \exp(-h_{s,t,j}) - \frac{\tau_{\epsilon,s}^2}{2} \right\} \delta, \tau_{\epsilon,s}^2 \delta\right) \quad (22)$$

for $j = 0, \dots, M - 1$, where $\delta = 1/M$.

We denote the parameter vector for the factor stochastic volatility model given by equations (16), (17) and either (19), (20) or (22) by

$$\boldsymbol{\omega} = (\boldsymbol{\beta}; (\phi_k, \tau_{f,k}), k = 1, \dots, K; (\alpha_s, \mu_s, \tau_{\epsilon,s}), s = 1, \dots, S).$$

Although the factor SV model can be written in state space form as in Section 2.1, it is more efficient to take advantage of the extra structure in the model and base the sampling scheme on multiple independent univariate state space models. The next section outlines the conditional independence structure in the factor SV model. Sections S4 and S5 of the supplement give the more complex target density and sampling schemes required for estimating the posterior distribution of the factor SV model.

Conditional independence in the factor SV model

The key to making the estimation of the factor SV model tractable is that the factor SV model in equation (16) separates into independent components consisting of K univariate SV models for the latent factors and S univariate state space models for the idiosyncratic errors given the values of $(\mathbf{y}_{1:T}, \mathbf{f}_{1:T}, \boldsymbol{\omega})$ and the conditional independence of the innovations of the returns. The sampling scheme generates the latent factors and factor loading matrix in PG steps and then, conditioning on the them, estimates a series of univariate state space models. For $k = 1, \dots, K$, we have that

$$f_{k,t} | \lambda_{k,t} \sim N(0, \exp(\lambda_{k,t})), \quad (23)$$

with the transition density in equation (17). For $s = 1, \dots, S$, we have

$$y_{s,t} | \mathbf{f}_t, h_{s,t} \sim N(\boldsymbol{\beta}_s \mathbf{f}_t, \exp(h_{s,t})), \quad (24)$$

with the exact and approximate transition densities given in equations (19), (20) or (22).

Section 4.2 shows on both simulated and real data that the PMMH+PG sampler works well. We note that our example merely illustrates our methods which can naturally handle multiple factors and most types of log-volatilities for both the factors and idiosyncratic errors.

4.2 Empirical Studies

This section presents empirical results for the factor SV model described in Section 4.1 to illustrate the flexibility of the sampling approach given in our article. Section 4.2.1 presents a simulation study for the factor SV model with the idiosyncratic log-volatilities following Gaussian OU processes with exact and approximate transition densities. Section 4.2.2 presents empirical results for the factor SV model with the idiosyncratic log-volatilities following Gaussian OU processes and GARCH diffusion processes using a sample of daily US industry stock returns data.

We use the same notation as Section 3.3 to describe the algorithms in this study. For example, the basic sampler, as used in Sampling Scheme 1, is PMMH(θ_1)+PG(θ_2) sampling the parameter vector θ_1 in the PMMH step and θ_2 in the PG step. Our general procedure to determine an efficient sampling scheme is to first run a PG algorithm to identify which parameters have large IACTs, or, in some cases, require a large amount of computational time to generate in the PG step. We then generate these parameters in the PMMH step.

4.2.1 Simulation Study

We conducted a simulation study for the factor SV model with the idiosyncratic log-volatilities following Gaussian OU continuous time volatility processes with exact and approximate transition densities.

We compare the performance of the samplers listed below. Section 3.3 gives the notation for the samplers. The samplers are: (I) PMMH($\boldsymbol{\alpha}, \boldsymbol{\tau}_\epsilon^2, \boldsymbol{\tau}_j^2$) +

PG ($\mathbf{f}_{1:T}, \boldsymbol{\beta}, \boldsymbol{\mu}, \phi$) for the Gaussian OU model with exact transition densities and PMMH ($\boldsymbol{\alpha}, \boldsymbol{\tau}_\epsilon^2, \boldsymbol{\tau}_f^2, \boldsymbol{\mu}$) + PG ($\mathbf{f}_{1:T}, \boldsymbol{\beta}, \phi$) for the Gaussian OU model with approximate transition densities, (II) PGAT ($\mathbf{f}_{1:T}, \boldsymbol{\beta}, \boldsymbol{\alpha}, \boldsymbol{\tau}_\epsilon^2, \boldsymbol{\mu}, \phi, \boldsymbol{\tau}_f^2$), (III) PGBS ($\mathbf{f}_{1:T}, \boldsymbol{\beta}, \boldsymbol{\alpha}, \boldsymbol{\tau}_\epsilon^2, \boldsymbol{\mu}, \phi, \boldsymbol{\tau}_f^2$), (IV) PMMH-RW ($\mathbf{f}_{1:T}, \boldsymbol{\beta}, \boldsymbol{\alpha}, \boldsymbol{\tau}_\epsilon^2, \boldsymbol{\mu}, \phi, \boldsymbol{\tau}_f^2$), (V) PMMH-MALA ($\mathbf{f}_{1:T}, \boldsymbol{\beta}, \boldsymbol{\alpha}, \boldsymbol{\tau}_\epsilon^2, \boldsymbol{\mu}, \phi, \boldsymbol{\tau}_f^2$), (VI) Corr. PMMH-RW ($\mathbf{f}_{1:T}, \boldsymbol{\beta}, \boldsymbol{\alpha}, \boldsymbol{\tau}_\epsilon^2, \boldsymbol{\mu}, \phi, \boldsymbol{\tau}_f^2$), (VII) Corr. PMMH-MALA ($\mathbf{f}_{1:T}, \boldsymbol{\beta}, \boldsymbol{\alpha}, \boldsymbol{\tau}_\epsilon^2, \boldsymbol{\mu}, \phi, \boldsymbol{\tau}_f^2$), (VIII) PGDA ($\mathbf{f}_{1:T}, \boldsymbol{\beta}, \boldsymbol{\alpha}, \boldsymbol{\tau}_\epsilon^2, \boldsymbol{\mu}, \phi, \boldsymbol{\tau}_f^2$). We first compare the three samplers PMMH+PG, PGAT, and PGBS and then discuss the PMMH and PGDA sampling schemes for the factor SV model.

We simulated data with $T = 1,000$ observations, $S = 20$ stocks, and $K = 1$ factors from the factor SV model in equation (16), setting $\alpha_s = 0.06$, and $\tau_{\epsilon,s}^2 = 0.1$ for all s , $\phi_1 = 0.98$, $\tau_{f,1}^2 = 0.1$ and $\beta_s = 0.8$ for all s . We chose independent Gaussian priors for every unrestricted element of the factor loading matrix $\boldsymbol{\beta}$, i.e. $\beta_{s,k} \sim N(0, 1)$. The priors for the state transition density parameters are $\alpha_s \sim IG\left(\frac{v_0}{2}, \frac{s_0}{2}\right)$, $\tau_{\epsilon,s}^2 \sim IG\left(\frac{v_0}{2}, \frac{s_0}{2}\right)$, $\tau_{f,k}^2 \sim IG\left(\frac{v_0}{2}, \frac{s_0}{2}\right)$, where $v_0 = 10$, $s_0 = 1$, and $\phi_k \sim U(-1, 1)$. These prior densities cover most possible values in practice. The initial state of $\lambda_{k,t}$ is assumed normally distributed $N\left(0, \frac{\tau_{f,k}^2}{1-\phi_k^2}\right)$, for $k = 1, \dots, K$. The initial state of $h_{s,t}$ is also assumed normally distributed $N\left(\mu_s, \frac{\tau_{\epsilon,s}^2}{2\alpha_s}\right)$, for $s = 1, \dots, S$. We ran all the sampling schemes for 11,000 iterations and discarded the initial 1,000 iterates as warmup. We used $M = 10$ latent points for the Euler approximations to the state transition densities.

Gaussian OU process with exact transition density

Table S1 in Section S6 of the supplement shows the IACT estimates for the parameters in the factor SV model estimated for three different samplers using the exact transition density, (I) PMMH ($\boldsymbol{\alpha}, \boldsymbol{\tau}_\epsilon^2, \boldsymbol{\tau}_f^2$) + PG ($\boldsymbol{\mu}, \boldsymbol{\beta}, \mathbf{f}_{1:T}, \phi$), (II) PGAT ($\mathbf{f}_{1:T}, \boldsymbol{\beta}, \boldsymbol{\alpha}, \boldsymbol{\tau}_\epsilon^2, \boldsymbol{\tau}_f^2, \phi$) and (III) PGBS ($\mathbf{f}_{1:T}, \boldsymbol{\beta}, \boldsymbol{\alpha}, \boldsymbol{\tau}_\epsilon^2, \boldsymbol{\tau}_f^2, \phi$). All three samplers estimate the factor loading matrix $\boldsymbol{\beta}$ and $\boldsymbol{\mu}$ with comparable IACT values. The PMMH+PG sampler always has lower IACT values than both PG samplers for the parameters $\boldsymbol{\alpha}$, $\boldsymbol{\tau}_\epsilon^2$, $\boldsymbol{\tau}_f^2$, and ϕ . There are some improvements in terms of IACT obtained by using PGBS compared to PGAT. Table 4 summarises the estimation results when the exact transition density is used and shows that in terms of TNV_{MAX} , the PMMH+PG sampler is 9.25 and 4.19 times better than PGAT and PGBS, respectively, and in terms of TNV_{MEAN} , the PMMH+PG is 2.69 and 2.55 times better than PGAT and PGBS, respectively.

Table 4: Comparing different samplers in terms of Time Normalised Variance (TNV) with the exact transition density used for the Gaussian OU model: Sampler I: PMMH $(\boldsymbol{\alpha}, \boldsymbol{\tau}_\epsilon^2, \boldsymbol{\tau}_f^2) + \text{PG}(\mathbf{f}_{1:T}, \boldsymbol{\beta}, \boldsymbol{\mu}, \phi)$, Sampler II: PGAT $(\mathbf{f}_{1:T}, \boldsymbol{\beta}, \boldsymbol{\alpha}, \boldsymbol{\tau}_\epsilon^2, \boldsymbol{\mu}, \phi, \boldsymbol{\tau}_f^2)$, sampler III: PGBS $(\mathbf{f}_{1:T}, \boldsymbol{\beta}, \boldsymbol{\alpha}, \boldsymbol{\tau}_\epsilon^2, \boldsymbol{\mu}, \phi, \boldsymbol{\tau}_f^2)$. The data was simulated with $T = 1000$, $S = 20$, and $K = 1$, and number of particles $N = 500$. Time denotes the time taken in seconds for one iteration of the method.

	<i>I</i>	<i>II</i>	<i>III</i>
$\widehat{\text{IACT}}_{\text{MAX}}$	18.07	283.23	101.64
TNV_{max}	33.97	314.39	142.30
RTNV_{max}	1	9.25	4.19
$\widehat{\text{IACT}}_{\text{MEAN}}$	8.54	38.96	29.26
TNV_{MEAN}	16.06	43.25	40.96
$\text{RTNV}_{\text{MEAN}}$	1	2.69	2.55
Time	1.88	1.11	1.40

Gaussian OU process with an Euler evolution transition density

Table S2 in Section S6 of the supplement shows the IACT values for all the parameters in the model for the three samplers, (I) PMMH $(\boldsymbol{\mu}, \boldsymbol{\alpha}, \boldsymbol{\tau}_\epsilon^2, \boldsymbol{\tau}_f^2) + \text{PG}(\boldsymbol{\beta}, \mathbf{f}_{1:T}, \phi)$, (II) PGAT $(\mathbf{f}_{1:T}, \boldsymbol{\beta}, \boldsymbol{\alpha}, \boldsymbol{\tau}_\epsilon^2, \boldsymbol{\tau}_f^2, \phi)$ and (III) PGBS $(\mathbf{f}_{1:T}, \boldsymbol{\beta}, \boldsymbol{\alpha}, \boldsymbol{\tau}_\epsilon^2, \boldsymbol{\tau}_f^2, \phi)$, using the Euler approximation scheme for the transition density. The table shows that the PMMH+PG samplers with the exact and approximate state transition densities have very similar IACT values for all the parameters suggesting that the inefficiency of the PMMH+PG sampler does not deteriorate when the Euler approximation is used. However, both PG samplers, PGAT and PGBS, using the Euler approximation are significantly worse than the PGAT and PGBS samplers with the exact transition density. For example, the IACT of τ_4^2 in PGAT with the exact transition density is 283.23, compared to 977.93 for PGAT with the Euler approximation.

Table 5 summarises the estimation results with the Euler approximation of the transition density and shows that in terms of TNV_{MAX} , the PMMH+PG sampler is 60.57 and 50.72 times better than PGAT and PGBS, respectively, and in terms of TNV_{MEAN} , the PMMH+PG sampler is 14.67 and 12.95 times better than the PGAT and PGBS samplers, respectively. Similarly to the univariate case in Section 3.3, we note that if Euler approximations are used for the state transition densities then all three samplers PMMH+PG, PGAT, and PGBT take approximately the same computing time because the PG samplers need to store and trace back all the latent log-volatilities $h_{s,t}$ and the M latent data points between t and $t + 1$ for all $s = 1, \dots, S$ and $t = 1, \dots, T$, whereas the PMMH+PG sampler only needs to store and trace back the latent log-volatilities $h_{s,t}$ for all $s = 1, \dots, S$ and $t = 1, \dots, T$.

Table 5: Comparing different samplers in terms of Time Normalised Variance using an Euler approximation for the state transition density for the Gaussian OU model: Sampler I: PMMH $(\boldsymbol{\alpha}, \boldsymbol{\tau}_\epsilon^2, \boldsymbol{\mu}, \boldsymbol{\tau}_f^2) + \text{PG}(\mathbf{f}_{1:T}, \boldsymbol{\beta}, \boldsymbol{\phi})$, Sampler II: PGAT $(\mathbf{f}_{1:T}, \boldsymbol{\beta}, \boldsymbol{\alpha}, \boldsymbol{\tau}_\epsilon^2, \boldsymbol{\mu}, \boldsymbol{\phi}, \boldsymbol{\tau}_f^2)$, sampler III: PGBS $(\mathbf{f}_{1:T}, \boldsymbol{\beta}, \boldsymbol{\alpha}, \boldsymbol{\tau}_\epsilon^2, \boldsymbol{\mu}, \boldsymbol{\phi}, \boldsymbol{\tau}_f^2)$ for the simulated data with $T = 1,000$, $S = 20$, and $K = 1$, and the number of particles $N = 1,000$. Time denotes the time taken in seconds for one iteration of the method.

	<i>I</i>	<i>II</i>	<i>III</i>
$\widehat{\text{IACT}}_{\text{MAX}}$	17.57	977.93	792.88
TNV_{max}	113.50	6874.85	5756.31
RTNV_{max}	1	60.57	50.72
$\widehat{\text{IACT}}_{\text{MEAN}}$	14.17	191.04	163.26
TNV_{MEAN}	91.54	1343.01	1185.27
$\text{RTNV}_{\text{MEAN}}$	1	14.67	12.95
Time	6.46	7.03	7.26

The PMMH and PGDA Sampling Schemes for the Factor SV Model

This section discusses the PMMH samplers, both the standard and correlated PMMH, and the PGDA sampler of Fearnhead and Meligkotsidou [2016] to estimate the factor SV model which are denoted by sampling schemes IV to VIII. The PMMH method generates the parameters by integrating out all the latent factors, so that the observation equation is given by

$$\mathbf{y}_t | \boldsymbol{\lambda}_t, \mathbf{h}_t, \boldsymbol{\omega} \sim N(\mathbf{0}, \boldsymbol{\beta} \mathbf{D}_t \boldsymbol{\beta}' + \mathbf{V}_t). \quad (25)$$

The state transition equations are given by equations (17) and either equation (19) for the closed form case or equation (20) for the Euler scheme for the OU model and equation (22) for the Euler scheme for the GARCH model. The PMMH method uses the observation density, which includes all $(K + S)$ dimensional latent log-volatilities simultaneously. This becomes a high dimensional (21 dimensional) state space model. The performance of the standard PMMH sampler depends critically on the number of particles N used to estimate the likelihood. Pitt et al. [2012] suggest selecting the number of particles N such that the variance of the log of the estimated likelihood is around 1 to obtain an optimal tradeoff between computing time and statistical efficiency. Table 6 gives the variance of the log of the estimated likelihood for different numbers of particles using the bootstrap filter and shows that even with 5,000 particles, the log of the estimated likelihood still has a large variance and the Markov chain for the standard PMMH approach (sampling schemes IV and V) would get stuck. We therefore do not report results for the standard PMMH method as it is computationally very expensive and its TNV would be significantly higher than the PG and PMMH+PG methods.

From Section 3.3, we need $\log(Z_{1:T}(\boldsymbol{\theta}', \mathbf{u}'))$ and $\log(Z_{1:T}(\boldsymbol{\theta}, \mathbf{u}))$ to be highly cor-

related to reduce the variance of the difference between them for the correlated PMMH method. We now set the correlation between the individual elements of \mathbf{u} and \mathbf{u}' to $\text{corr}(u_i, u'_i) = 0.999999$. We then obtained 1,000 independent estimates of $\log(Z_{1:T}(\boldsymbol{\theta}, \mathbf{u}'))$ and $\log(Z_{1:T}(\boldsymbol{\theta}, \mathbf{u}))$ at the true value of $\boldsymbol{\theta}$ and computed their sample correlation. The sample correlation was 0.06, showing that it is difficult to preserve the correlation in such a high dimensional state space model and that the correlated PMMH Markov chain would still get stuck unless enough particles are used to ensure that the variance of the log of the estimator of the likelihood is close to 1.

A second problem with the PMMH approach is the large number of parameters to be estimated. Constructing proposals in high dimensions is remarkably difficult, and often requires estimating gradients and Hessian matrices. On the other hand, simpler approaches such as the adaptive random walk are very inefficient in large dimensions, as we showed in Section 3.3. Hence, it is natural to use a parameter splitting strategy and hybrid samplers.

Finally, we do not report results for the PGDA method applied to the factor stochastic volatility model as it is very clear that its TNV would be significantly higher than the PMMH+PG method. This sampler updates pseudo observations of the parameters by MCMC and updates the latent states and parameters jointly using a particle filter. Section 3.3 shows that this sampler does not work well when the model has many parameters. Note that Fearnhead and Meligkotsidou [2016] only apply their method to a simple univariate SV model. The factor SV model considered in this section is more complex with a large number of parameters and high dimensional latent states.

Table 6: The Variance of the log of the estimated likelihood for the PMMH method with the exact transition density for different numbers of particles for the simulated dataset with $T = 1,000$, $S = 20$, and $K = 1$ evaluated at the true values of the parameters. CPU time to estimate the likelihood is in seconds .

Number of Particles	Variance of log-likelihood	CPU time
250	1672.07	4.39
500	766.38	8.57
2500	331.65	45.03
5000	243.82	130.53

4.2.2 Application to US stock returns

We now apply our methods to a sample of daily US industry stock returns data. The data, obtained from the Kenneth French website² consists of daily returns for $S = 20$ value-weighted industry portfolios, using a sample from January 3rd, 2001 to the 24th of December, 2003, a total of 1,000 observations.

We compare the PMMH+PG, PGAT, and PGBS samplers for the factor SV model with the idiosyncratic log-volatilities following Gaussian OU processes with exact and approximate

² <http://mba.tuck.dartmouth.edu/pages/faculty/ken.french/datalibrary.html>

transition densities and GARCH diffusion processes and show that the performance of the PMMH+PG sampler does not deteriorate for the real data, whereas both PGAT and PGBS samplers get worse in terms of the IACT values of the parameters, especially with the Euler approximation. This section does not compare the PMMH+PG sampler with either of the standard or correlated PMMH samplers or the PGDA sampler because of the problems discussed in Section 4.2.1.

Gaussian OU process with exact and Euler evolution transition densities

This section compares the following samplers: (I) PMMH $(\boldsymbol{\alpha}, \tau_\epsilon^2, \tau_f^2) + \text{PG}(\mathbf{f}_{1:T}, \boldsymbol{\beta}, \boldsymbol{\mu}, \phi)$ for the Gaussian OU model with exact transition densities and PMMH $(\boldsymbol{\alpha}, \tau_\epsilon^2, \tau_f^2, \boldsymbol{\mu}) + \text{PG}(\mathbf{f}_{1:T}, \boldsymbol{\beta}, \phi)$ for the Gaussian OU model with approximate transition densities, (II) PGAT $(\mathbf{f}_{1:T}, \boldsymbol{\beta}, \boldsymbol{\alpha}, \tau_\epsilon^2, \boldsymbol{\mu}, \phi, \tau_f^2)$, and (III) PGBS $(\mathbf{f}_{1:T}, \boldsymbol{\beta}, \boldsymbol{\alpha}, \tau_\epsilon^2, \boldsymbol{\mu}, \phi, \tau_f^2)$ for the factor SV model with the idiosyncratic log-volatilities following Gaussian OU processes with exact and approximate transition densities. Tables S3 and S4 in Section S6 of the supplement show the IACT estimates for all the parameters in the factor SV model estimated with exact transition densities for the Gaussian OU model and Euler approximations for the transition densities for the Gaussian OU processes. As for the simulated data, all three samplers estimate the factor loading matrix $\boldsymbol{\beta}$ and $\boldsymbol{\mu}$ efficiently and with comparable IACT values. The performance of the PMMH+PG sampler does not deteriorate for the real data, whereas both PGAT and PGBS samplers get worse in terms of the IACT values of the parameters, especially for the Euler approximation model. Overall, the PMMH+PG samplers always have smaller IACT values than both the PGAT and PGBS samplers for all the state transition parameters.

Tables 7 and 8 summarise the estimation results for the Gaussian OU model and show that in terms of TNV_{MAX} , the PMMH+PG sampler is 20.87 and 13.91 times better than the PGAT and PGBS samplers with the exact transition density, respectively, and the PMMH+PG sampler is 53.94 and 58.71 times, respectively, better than the PGAT and PGBS with the Euler approximation. In terms of TNV_{MEAN} , the PMMH+PG sampler is 5.61 and 4.73 times better than the PGAT and PGBS samplers with the exact transition density, respectively, and the PMMH+PG sampler is 22.17 and 22.40 times, respectively, better than the PGAT and PGBS samplers when using the Euler approximation.

Figures S1 and S2 in Section S6 of the supplement present the kernel density estimates of marginal posterior densities of four representative α and τ_ϵ^2 parameters, respectively, for the US stock returns data. The density estimates are for PMMH+PG using exact and approximate transition densities and PG with approximate transition densities using ancestral tracing and backward simulation for the Gaussian OU model. The figures show that both PMMH+PG samplers produce estimates that are close to each other, whereas the PG samplers are much less reliable and suggest that the PG estimators did not converge. This confirms the usefulness of the PMMH+PG samplers for this class of model.

Table 7: Comparing different samplers in terms of Time Normalised Variance with the exact transition density for the Gaussian OU model: Sampler I: PMMH $(\boldsymbol{\alpha}, \tau_\epsilon^2, \tau_f^2) + \text{PG}(\mathbf{f}_{1:T}, \boldsymbol{\beta}, \boldsymbol{\mu}, \boldsymbol{\phi})$, Sampler II: PGAT $(\mathbf{f}_{1:T}, \boldsymbol{\beta}, \boldsymbol{\alpha}, \tau_\epsilon^2, \boldsymbol{\mu}, \boldsymbol{\phi}, \tau_f^2)$, sampler III: PGBS $(\mathbf{f}_{1:T}, \boldsymbol{\beta}, \boldsymbol{\alpha}, \tau_\epsilon^2, \boldsymbol{\mu}, \boldsymbol{\phi}, \tau_f^2)$ for US stock returns data with $T = 1,000$, $S = 20$, and $K = 1$, and number of particles $N = 500$. Time denotes the time taken in seconds for one iteration of the method.

	<i>I</i>	<i>II</i>	<i>III</i>
$\widehat{\text{IACT}}_{\text{MAX}}$	20.57	682.49	382.86
TNV_{max}	38.26	798.51	532.18
RTNV_{max}	1	20.87	13.91
$\widehat{\text{IACT}}_{\text{MEAN}}$	8.54	76.19	54.06
TNV_{MEAN}	15.88	89.14	75.14
$\text{RTNV}_{\text{MEAN}}$	1	5.61	4.73
Time	1.86	1.17	1.39

Table 8: Comparing different samplers in terms of Time Normalised Variance with the Euler approximation for state transition density for the Gaussian OU model: Sampler I: PMMH $(\boldsymbol{\alpha}, \tau_\epsilon^2, \boldsymbol{\mu}, \tau_f^2) + \text{PG}(\mathbf{f}_{1:T}, \boldsymbol{\beta}, \boldsymbol{\phi})$, Sampler II: PGAT $(\mathbf{f}_{1:T}, \boldsymbol{\beta}, \boldsymbol{\alpha}, \tau_\epsilon^2, \boldsymbol{\mu}, \boldsymbol{\phi}, \tau_f^2)$, sampler III: PGBS $(\mathbf{f}_{1:T}, \boldsymbol{\beta}, \boldsymbol{\alpha}, \tau_\epsilon^2, \boldsymbol{\mu}, \boldsymbol{\phi}, \tau_f^2)$ with backward simulation for US stock returns data with $T = 1,000$, $S = 20$, and $K = 1$, and number of particles $N = 1,000$. Time denotes the time taken in seconds for one iteration of the method.

	<i>I</i>	<i>II</i>	<i>III</i>
$\widehat{\text{IACT}}_{\text{MAX}}$	23.99	1215.77	1228.99
TNV_{max}	152.82	8242.92	8971.63
RTNV_{max}	1	53.94	58.71
$\widehat{\text{IACT}}_{\text{MEAN}}$	12.99	270.58	253.90
TNV_{MEAN}	82.75	1834.53	1853.47
$\text{RTNV}_{\text{MEAN}}$	1	22.17	22.40
Time	6.37	6.78	7.30

GARCH diffusion process with an Euler evolution transition density

This section compares the following samplers: (I) PMMH $(\boldsymbol{\alpha}, \tau_\epsilon^2, \tau_f^2, \boldsymbol{\mu}) + \text{PG}(\mathbf{f}_{1:T}, \boldsymbol{\beta}, \boldsymbol{\phi})$, (II) PGAT $(\mathbf{f}_{1:T}, \boldsymbol{\beta}, \boldsymbol{\alpha}, \tau_\epsilon^2, \boldsymbol{\mu}, \boldsymbol{\phi}, \tau_f^2)$, and (III) PGBS $(\mathbf{f}_{1:T}, \boldsymbol{\beta}, \boldsymbol{\alpha}, \tau_\epsilon^2, \boldsymbol{\mu}, \boldsymbol{\phi}, \tau_f^2)$ for the factor SV model with the idiosyncratic log-volatilities following GARCH diffusion processes which do not have closed form state transition densities.

Table S5 in Section S6 of the supplement shows the IACT estimates for all the parameters for the factor SV model with the idiosyncratic log-volatilities following GARCH diffusion processes which do not have closed form state transition densities. As for the models with Gaussian OU processes, all three samplers estimate the factor loading matrix $\boldsymbol{\beta}$ efficiently

and with comparable IACT values. The performance of the PMMH+PG sampler does not deteriorate for the real data, whereas both the PGAT and PGBS samplers get worse in terms of the IACT values for the remaining parameters. Overall, the PMMH+PG sampler always has smaller IACT values than both the PGAT and PGBS samplers for all the state transition parameters.

Table 9 summarises the estimation results for the GARCH diffusion model and shows that in terms of TNV_{MAX} , the PMMH+PG is 19.56 and 22.11 times better than PGAT and PGBS samplers. In terms of TNV_{MEAN} , the PMMH+PG is 25.84 and 28.01 times better than PGAT and PGBS, respectively. This confirms the usefulness of the PMMH+PG samplers for this class of the model.

Table 9: Comparing different samplers in terms of Time Normalised Variance with the Euler approximation for the state transition density for the GARCH diffusion model. Sampler I: PMMH $(\boldsymbol{\alpha}, \boldsymbol{\tau}_\epsilon^2, \boldsymbol{\mu}, \boldsymbol{\tau}_f^2) + \text{PG}(\mathbf{f}_{1:T}, \boldsymbol{\beta}, \boldsymbol{\phi})$, Sampler II: PGAT $(\mathbf{f}_{1:T}, \boldsymbol{\beta}, \boldsymbol{\alpha}, \boldsymbol{\tau}_\epsilon^2, \boldsymbol{\mu}, \boldsymbol{\phi}, \boldsymbol{\tau}_f^2)$, Sampler III: PGBS $(\mathbf{f}_{1:T}, \boldsymbol{\beta}, \boldsymbol{\alpha}, \boldsymbol{\tau}_\epsilon^2, \boldsymbol{\mu}, \boldsymbol{\phi}, \boldsymbol{\tau}_f^2)$ for US stock returns data with $T = 1000$, $S = 20$, and $K = 1$, and number of particles $N = 1000$. Time denotes the time taken in seconds for one iteration of the method.

	<i>I</i>	<i>II</i>	<i>III</i>
$\widehat{\text{IACT}}_{MAX}$	147.16	3098.27	3257.52
TNV_{MAX}	1392.13	27233.79	30783.56
$RTNV_{MAX}$	1	19.56	22.11
$\widehat{\text{IACT}}_{MEAN}$	17.38	483.37	487.28
TNV_{MEAN}	164.41	4248.82	4604.80
$RTNV_{MEAN}$	1	25.84	28.01
Time	9.46	8.79	9.45

5 Discussion

Our article introduces a flexible particle Markov chain Monte Carlo sampling scheme for state space models where some parameters are generated without conditioning on the states (PMMH) while other parameters are generated conditional on the states (PG). Previous sampling schemes used PMMH or PG exclusively without combining both strategies. The technical contribution of our article is to set out the required particle framework for the flexible sampler and to obtain uniform ergodicity under given assumptions. Our examples demonstrate that it is advantageous to use this flexible sampling scheme to generate the parameters that are highly correlated with the states without conditioning on the states (the PMMH component) while the other parameters are generated by particle Gibbs (PG).

As we note in the introduction, in general, there are likely to be a number of different sampling schemes that can solve the same problems addressed in our article, and which sampler is best depends on a number of factors such as the model, the data set and the number of observations. We also note that our PMMH + PG approach can be further refined

by using the data augmented PMMH and PG sampling schemes proposed by Fearnhead and Meligkotsidou [2016] and the refined proposals for the PMMH sampling scheme by Dahlin et al. [2015] and Nemeth et al. [2016b].

Acknowledgement

The work of the authors was partially supported by an ARC Research Council Grant DP120104014. The work of Robert Kohn and David Gunawan was also partially supported by the ARC Center of Excellence grant CE140100049

References

- C. Andrieu and G. O. Roberts. The pseudo-marginal approach for efficient Monte Carlo computations. *The Annals of Statistics*, 37(2):697–725, 2009.
- C. Andrieu and M. Vihola. Convergence properties of pseudo-marginal Markov chain Monte Carlo algorithms. *Annals of Applied Probability*, 25(2):1030–1077, 2015.
- C. Andrieu, A. Doucet, and R. Holenstein. Particle Markov chain Monte Carlo methods. *Journal of the Royal Statistical Society, Series B*, 72(3):269–342, 2010.
- A. F. Brix, A. Lunde, and W. Wei. A general Schwartz model for energy spot price - estimation using a particle MCMC method. *Energy Economics*, 72:560–582, 2018.
- C. Carter and R. Kohn. Markov chain Monte Carlo in conditionally Gaussian state space models. *Biometrika*, 83(3):589–601, 1996.
- S. Chib, M. K. Pitt, and N. Shephard. Likelihood based inference for diffusion driven models. *Working Paper*, 2004.
- S. Chib, F. Nardari, and N. Shephard. Analysis of high dimensional multivariate stochastic volatility models. *Journal of Econometrics*, 134(2):341–371, 2006.
- N. Chopin and S. S. Singh. On the particle Gibbs sampler. *Bernoulli*, 21(3):1855–1883, 2015.
- J. Dahlin, F. Lindsten, and T. Schön. Particle Metropolis–Hastings using gradient and Hessian information. *Statistics and Computing*, 25(1):81–92, 2015.
- G. Deligiannidis, A. Doucet, and M. K. Pitt. The correlated pseudo-marginal method. *Journal of Royal Statistical Society, Series B*, 80(5):839–870, 2018.
- R. Douc and O. Cappé. Comparison of resampling schemes for particle filtering. In *Image and Signal Processing and Analysis, 2005. ISPA 2005. Proceedings of the 4th International Symposium on*, pages 64–69. IEEE, 2005.

- A. Doucet, S. Godsill, and C. Andrieu. On sequential Monte Carlo sampling methods for Bayesian filtering. *Statistics and Computing*, 10(3):197–208, 2000.
- J. Durbin and S. Koopman. *Time series analysis of state space methods*. Oxford University Press, second edition, 2012.
- P. Fearnhead and L. Meligkotsidou. Augmentation schemes for particle MCMC. *Statistics and Computing*, 26(6):1293–1306, 2016.
- R. Gerlach, C. Carter, and R. Kohn. Efficient Bayesian inference for dynamic mixture models. *Journal of the American Statistical Association*, 95(451):819–828, 2000.
- J. F. Geweke and G. Zhou. Measuring the pricing error of the arbitrage pricing theory. *Review of Financial Studies*, 9(2):557–587, 1996.
- S. Godsill, A. Doucet, and M. West. Monte Carlo smoothing for nonlinear time series. *Journal of the American Statistical Association*, 99(465):156–168, 2004.
- D. Guo, X. Wang, and R. Chen. New sequential Monte Carlo methods for nonlinear dynamic systems. *Statistics and computing*, 15(2):135–147, 2005.
- K. Ignatieva, P. Rodrigues, and N. Seeger. Empirical analysis of affine versus nonaffine variance specifications in jump-diffusion models for equity indices. *Journal of Business and Economic Statistics*, 33(1):68–75, 2015.
- G. Kastner, S. Fruhwirth-Schnatter, and H. F. Lopes. Efficient Bayesian inference for multivariate factor stochastic volatility models. *Journal of Computational and Graphical Statistics*, 26(4):905–917, 2017.
- S. Kim, N. Shephard, and S. Chib. Stochastic volatility: likelihood inference and comparison with ARCH models. *The Review of Economic Studies*, 65(3):361–393, 1998.
- G. Kitagawa. Monte Carlo filter and smoother for non-Gaussian nonlinear state space models. *Journal of Computational and Graphical Statistics*, 5(1):1–25, 1996.
- T. S. Kleppe, J. Yu, and H. Skaug. Estimating the GARCH diffusion: Simulated maximum likelihood in continuous time. *SMU Economics and Statistics Working Paper Series*, 13, 2010.
- F. Lindsten and T. B. Schön. On the use of backward simulation in particle Markov chain Monte Carlo methods. arxiv:1110.2873, 2012a.
- F. Lindsten and T. B. Schön. On the use of backward simulation in the particle Gibbs sampler. In *Proceedings of the 37th International Conference on Acoustics, Speech, and Signal Processing*, pages 3845–3848. ICASSP, 2012b.
- F. Lindsten and T. B. Schon. Backward simulation methods for Monte Carlo statistical inference. *Foundations and Trends in Machine Learning*, 6(1):1–143, 2013.

- F. Lindsten, M. I. Jordan, and T. B. Schön. Particle Gibbs with ancestor sampling. *Journal of Machine Learning Research*, 15:2145–2184, 2014.
- F. Lindsten, P. Bunch, S. S. Singh, and T. B. Schön. Particle ancestor sampling for near-degenerate or intractable state transition models. arxiv:1505.0635v1, 2015.
- C. Nemeth, P. Fearnhead, and L. Mihaylova. Particle approximations of the score and observed information matrix for parameter estimation in state-space models with linear computational cost. *Journal of Computational and Graphical Statistics*, 25(4):1138–1157, 2016a.
- C. Nemeth, C. Sherlock, and P. Fearnhead. Particle Metropolis-adjusted Langevin algorithms. *Biometrika*, 103(3):701–717, 2016b.
- J. Olsson and T. Ryden. Rao-Blackwellization of particle Markov chain Monte Carlo methods using forward filtering backward sampling. *IEEE Transactions on Signal Processing*, 59(10):4606–4619, 2011.
- M. K. Pitt, R. d. S. Silva, P. Giordani, and R. Kohn. On some properties of Markov chain Monte Carlo simulation methods based on the particle filter. *Journal of Econometrics*, 171(2):134–151, 2012.
- G. O. Roberts and J. S. Rosenthal. General state space Markov chains and MCMC algorithms. *Probability Surveys*, 1:20–71, 2004.
- G. O. Roberts and J. S. Rosenthal. Examples of adaptive MCMC. *Journal of Computational and Graphical Statistics*, 18(2):349–367, 2009.
- E. Stein and J. Stein. Stock price distributions with stochastic volatility: an analytic approach. *Review of Financial Studies*, 4:727–752, 1991.
- O. Stramer and M. Bognar. Bayesian inference for irreducible diffusion processes using the pseudo-marginal approach. *Bayesian Analysis*, 6(2):231–258, 2011.
- R. Van Der Merwe, A. Doucet, N. De Freitas, and E. Wan. The unscented particle filter. *Advances in neural information processing systems*, pages 584–590, 2001.
- X. Wu, G. Zhou, and S. Wang. Estimation of market prices of risks in the G.A.R.C.H. diffusion model. *Economic Research-Ekonomska Istraživanja*, 31(1):15–36, 2018.

Online Supplement for “A Flexible Particle Markov chain Monte Carlo method”

We use the following notation in the supplement. Equation (1), Algorithm 1, and Sampling Scheme 1, etc, refer to the main paper, while equation (S1), Algorithm S1, and Sampling Scheme S1, etc, refer to the supplement. Section S1 lists some of the algorithms used in the main paper. These algorithms are used in Andrieu et al. [2010] and are included here for notational consistency. Section S2 discusses the convergence of Sampling Scheme 1 to its target distribution. Section S3 discusses other choices of target distribution and how it is straightforward to modify the results in the main paper to apply to these distributions. Section S4 discusses the target density of the PMMH+PG sampler for the multivariate factor SV model. Section S5 discusses the PMMH+PG sampling schemes for the factor SV model. Section S6 presents some additional tables and plots based on the analysis reported in Sections 4.2.1 and 4.2.2.

S1 Algorithms

The Sequential Monte Carlo algorithm used here is the same one as in Andrieu et al. [2010] and is defined as follows.

Algorithm S1 (Sequential Monte Carlo)

1. For $t = 1$:

(a) Sample X_1^i from $m_1^\theta(x)$, for $i = 1, \dots, N$

(b) Calculate the importance weights

$$w_1^i = \frac{f_1^\theta(x_1^i) g_\theta(y_1|x_1^i)}{m_1^\theta(x_1^i)} \quad (i = 1, \dots, N),$$

and normalize them to obtain $\bar{w}_1^{1:N}$.

2. For $t = 2, 3, \dots$:

(a) Sample the ancestral indices $A_{t-1}^{1:N} \sim \mathcal{M}(a_{t-1}^{1:N}|\bar{w}_{t-1}^{1:N})$

(b) Sample X_t^i from $m_t^\theta(x|x_{t-1}^{a_{t-1}^i})$, $i = 1, \dots, N$

(c) Calculate the importance weights

$$w_t^i = \frac{f_\theta(x_t^i|x_{t-1}^{a_{t-1}^i}) g_\theta(y_t|x_t^i)}{m_t^\theta(x_t^i|x_{t-1}^{a_{t-1}^i})} \quad (i = 1, \dots, N)$$

and normalize them to obtain $\bar{w}_t^{1:N} = w_t^{1:N} / \sum_{i=1}^N w_t^i$.

Algorithm S2 is the conditional sequential Monte Carlo algorithm (as in Andrieu et al. [2010]), consistent with $(x_{1:T}^j, a_{1:T-1}^j, j)$.

Algorithm S2 (Conditional Sequential Monte Carlo)

1. Fix $X_{1:T}^j = x_{1:T}^j$ and $A_{1:T-1}^j = b_{1:T-1}^j$.
2. For $t = 1$
 - (a) Sample X_1^i from $m_1^\theta(x)dx$, for $i \in \{1, \dots, N\} \setminus \{b_1^j\}$.
 - (b) Calculate the importance weights

$$w_1^i = \frac{f_1^\theta(x_1^i) g_\theta(y_1|x_1^i)}{m_1^\theta(x_1^i)} \quad (i = 1, \dots, N),$$

and normalize them to obtain $\bar{w}_1^{1:N}$.

3. For $t = 2, \dots, T$
 - (a) Sample the ancestral indices
$$A_{t-1}^{-(b_t^j)} \sim \mathcal{M} \left(a^{(-b_t^j)} | \bar{w}_{t-1}^{1:N} \right).$$
 - (b) Sample X_t^i from $m_t^\theta \left(x | x_{t-1}^{a_{t-1}^i} \right) dx$, $i \in \{1, \dots, N\} \setminus \{b_t^j\}$.
 - (c) Calculate the importance weights

$$w_t^i = \frac{f_\theta \left(x_t^i | x_{t-1}^{a_{t-1}^i} \right) g_\theta \left(y_t | x_t^i \right)}{m_t^\theta \left(x_t^i | x_{t-1}^{a_{t-1}^i} \right)} \quad (i = 1, \dots, N)$$

and normalized them to obtain $\bar{w}_t^{1:N}$.

S2 Ergodicity

This section discusses the assumptions required for the particle filter. We then discuss convergence of Sampling Scheme 1 in total variation norm and then consider the stronger condition of uniform convergence.

We will use the generalization of Sampling Scheme 1 to the case where there may be multiple PMMH steps and there may be multiple Gibbs steps. This was discussed in Section 2.4. Let $\theta := (\theta_1, \dots, \theta_p)$ be a partition of the parameter vector into p components where each component may be a vector and let $0 \leq p_1 \leq p$. Let $\Theta = \Theta_1 \times \dots \times \Theta_p$ be the corresponding partition of the parameter space. We use the notation $\theta_{-i} := (\theta_1, \dots, \theta_{i-1}, \theta_{i+1}, \dots, \theta_p)$. Sampling Scheme S2 generates the parameters $\theta_1, \dots, \theta_{p_1}$ using PMMH steps and the parameters $\theta_{p_1+1}, \dots, \theta_p$ using PG steps. To simplify the discussion, we assume that both particle marginal Metropolis-Hastings steps and particle Gibbs steps are used, i.e., $0 < p_1 < p$.

Sampling Scheme S2 (PMMH+PG Sampler) Given initial values for $U_{1:T}$, J and θ , one iteration of the MCMC involves the following steps.

1. (PMMH sampling) For $i = 1, \dots, p_1$

Step i :

- (a) Sample $\theta_i^* \sim q_{i,1}(\cdot | U_{1:T}, J, \theta_{-i}, \theta_i)$.
- (b) Sample $U_{1:T}^* \sim \psi(\cdot | \theta_{-i}, \theta_i^*)$.
- (c) Sample $J^* \sim \tilde{\pi}^N(\cdot | U_{1:T}^*, \theta_{-i}, \theta_i^*)$.
- (d) Set $(\theta_i, U_{1:T}, J) \leftarrow (\theta_i^*, U_{1:T}^*, J^*)$ with probability

$$\alpha_i(U_{1:T}, J, \theta_i; U_{1:T}^*, J^*, \theta_i^* | \theta_{-i}) = 1 \wedge \frac{\tilde{\pi}^N(U_{1:T}^*, \theta_i^* | \theta_{-i}) q_i(U_{1:T}, \theta_i | U_{1:T}^*, J^*, \theta_{-i}, \theta_i^*)}{\tilde{\pi}^N(U_{1:T}, \theta_i | \theta_{-i}) q_i(U_{1:T}^*, \theta_i^* | U_{1:T}, J, \theta_{-i}, \theta_i)}, \quad (\text{S1})$$

where

$$q_i(U_{1:T}^*, \theta_i^* | U_{1:T}, J, \theta_{-i}, \theta_i) = q_{i,1}(\theta_i^* | U_{1:T}, J, \theta_{-i}, \theta_i) \psi(U_{1:T}^* | \theta_{-i}, \theta_i^*).$$

2. (PG sampling) For $i = p_1 + 1, \dots, p$

Step i :

- (a) Sample $\theta_i^* \sim q_i(\cdot | X_{1:T}^J, B_{1:T-1}^J, J, \theta_{-i}, \theta_i)$.
- (b) Set $\theta_i \leftarrow \theta_i^*$ with probability

$$\alpha_i(\theta_i; \theta_i^* | X_{1:T}^J, B_{1:T-1}^J, J, \theta_{-i}) = 1 \wedge \frac{\tilde{\pi}^N(\theta_i^* | X_{1:T}^J, B_{1:T-1}^J, J, \theta_{-i})}{\tilde{\pi}^N(\theta_i | X_{1:T}^J, B_{1:T-1}^J, J, \theta_{-i})} \times \frac{q_i(\theta_i | X_{1:T}^J, B_{1:T-1}^J, J, \theta_{-i}, \theta_i^*)}{q_i(\theta_i^* | X_{1:T}^J, B_{1:T-1}^J, J, \theta_{-i}, \theta_i)}. \quad (\text{S2})$$

3. Sample $U_{1:T}^{(-J)} \sim \tilde{\pi}^N(\cdot | X_{1:T}^J, B_{1:T-1}^J, J, \theta)$ using the conditional sequential Monte Carlo algorithm (CSMC) discussed in Section 2.3.

4. Sample $J \sim \tilde{\pi}^N(\cdot | U_{1:T}, \theta)$.

We now discuss the assumptions required for the particle filter. For $t \geq 1$, we define,

$$S_t^\theta = (\mathbf{x}_{1:t} \in \mathcal{X}^t : \pi(\mathbf{x}_{1:t} | \theta) > 0) \quad \text{and} \quad Q_t^\theta = \{\mathbf{x}_{1:t} \in \mathcal{X}^t : \pi(\mathbf{x}_{1:t-1} | \theta) m_t^\theta(\mathbf{x}_t | \mathbf{x}_{1:t-1}, \mathbf{y}_{1:t}) > 0\}.$$

Assumption S1 ensures that the proposal densities $\pi(\mathbf{x}_{1:t-1} | \theta) m_t^\theta(\mathbf{x}_t | \mathbf{x}_{1:t-1}, \mathbf{y}_{1:t})$ can be used to approximate $\pi(\mathbf{x}_{1:t} | \theta)$ for $t \geq 1$.

Assumption S1 [Andrieu et al., 2010] We assume that $S_t^\theta \subseteq Q_t^\theta$ for any $\theta \in \Theta$ and $t = 1, \dots, T$

Assumption S1 is always satisfied in our implementation because we use the bootstrap filter with $p(\mathbf{x}_t|\mathbf{x}_{t-1}, \boldsymbol{\theta})$ as a proposal density which are positive everywhere.

We also require Assumption S2 given below.

Assumption S2 [Andrieu et al., 2010] For any $k = 1, \dots, N$ and $t = 1, \dots, T$, the resampling scheme $\mathcal{M}(a_{t-1}^{1:N}|\bar{w}_{t-1}^{1:N})$ satisfies $\mathcal{M}(a_{t-1}^k = j|\bar{w}_{t-1}^{1:N}) = \bar{w}_{t-1}^j$.

Assumption S2 is satisfied by the popular resampling schemes, such as multinomial, systematic, residual resampling.

Under Assumption S2, it is straightforward to show that the algorithm samples from the target density of the random variable $U_{1:T}^{(-J)} = \left(X_1^{(-B_1^J)}, \dots, X_T^{(-B_T^J)}, A_1^{(-B_2^J)}, \dots, A_{T-1}^{(-B_T^J)}\right)$, conditional on $U_{1:T}^J$ and index J given by

$$\tilde{\pi}^N \left(u_{1:T}^{(-j)} | x_{1:T}, b_{1:T-1}, j, \theta \right) = \frac{\psi(u_{1:T} | \theta)}{m_1^\theta(x_1^{b_1}) \prod_{t=2}^T \bar{w}_{t-1}^{a_{t-1}^i} m_t^\theta \left(x_t^{b_t} | x_{t-1}^{a_{t-1}^{b_t}} \right)};$$

see Andrieu et al. [2010] for details.

We now discuss convergence of Sampling Scheme S2 in total variation norm and then consider the stronger condition of uniform convergence. Note that, by construction, Sampling Scheme S2 has the stationary distribution

$$\tilde{\pi}^N \left(x_{1:T}, b_{1:T-1}, j, u_{1:T}^{(-j)}, \theta \right)$$

defined in (3). From Roberts and Rosenthal [2004] Theorem 4, irreducibility and aperiodicity are sufficient conditions for the Markov chain obtained using Sampling Scheme S2 to converge to its stationary distribution in total variation norm for $\tilde{\pi}^N$ -almost all starting values. These conditions must be checked for a particular sampler and it is often straightforward to do so. We will relate Sampling Scheme S2 to the particle Metropolis within Gibbs sampling scheme defined below.

Sampling Scheme S3 (Ideal) Given initial values for $U_{1:T}$, J and θ , one iteration of the MCMC sampling scheme involves the following steps

1. (PMMH sampling) For $i = 1, \dots, p_1$

Step i :

(a) Sample $\theta_i^* \sim q_{i,1}(\cdot | U_{1:T}, J, \theta_{-i}, \theta_i)$.

(b) Sample $(J^*, U_{1:T}^*) \sim \tilde{\pi}^N(\cdot | \theta_{-i}, \theta_i^*)$.

(c) Set $(\theta_i, U_{1:T}, J) \leftarrow (\theta_i^*, U_{1:T}^*, J^*)$ with probability

$$\begin{aligned} \tilde{\alpha}_i(U_{1:T}, J, \theta_i; U_{1:T}^*, J^*, \theta_i^* | \theta_{-i}) = \\ 1 \wedge \frac{\tilde{\pi}^N(\theta_i^* | \theta_{-i})}{\tilde{\pi}^N(\theta_i | \theta_{-i})} \frac{q_{i,1}(\theta_i | U_{1:T}^*, J^*, \theta_{-i}, \theta_i^*)}{q_{i,1}(\theta_i^* | U_{1:T}, J, \theta_{-i}, \theta_i)} \end{aligned} \quad (\text{S3})$$

2. (PG sampling) For $i = p_1 + 1, \dots, p$

Step i :

(a) Sample $\theta_i^* \sim q_i(\cdot | X_{1:T}^J, B_{1:T-1}^J, J, \theta_{-i}, \theta_i)$.

(b) Set $\theta_i \leftarrow \theta_i^*$ with probability

$$\begin{aligned} \alpha_i \{ \theta_i; \theta_i^* | X_{1:T}^J, B_{1:T-1}^J, J, \theta_{-i} \} = \\ 1 \wedge \frac{\tilde{\pi}^N(\theta_i^* | X_{1:T}^J, B_{1:T-1}^J, J, \theta_{-i})}{\tilde{\pi}^N(\theta_i | X_{1:T}^J, B_{1:T-1}^J, J, \theta_{-i})} \\ \frac{q_i(\theta_i | X_{1:T}^J, B_{1:T-1}^J, J, \theta_{-i}, \theta_i^*)}{q_i(\theta_i^* | X_{1:T}^J, B_{1:T-1}^J, J, \theta_{-i}, \theta_i)}. \end{aligned} \quad (\text{S4})$$

3. Sample $U_{1:T}^{(-J)} \sim \tilde{\pi}^N(\cdot | X_{1:T}^J, B_{1:T-1}^J, J, \theta)$ using Algorithm S2.

4. Sample $J \sim \tilde{\pi}^N(\cdot | U_{1:T}, \theta)$.

We call Sampling Scheme S3 an *ideal* particle sampling scheme because in Part 1 Step i(b) it generates the particles $U_{1:T}^*$ from their conditional distribution $\tilde{\pi}^N(\cdot | \theta_{-i}, \theta_i^*)$ instead of using a Metropolis-Hastings proposal. Thus comparing Sampling Schemes S2 and S3 allows us to concentrate on the effect of the Metropolis-Hastings proposal for the particles on the convergence of the sampler.

Remark S3 *Andrieu and Roberts [2009] and Andrieu and Vihola [2015] discuss the relationship between PMMH sampling schemes with one block of parameters and an ideal Metropolis-Hastings sampling scheme not involving the particles. Sampling Schemes S2 and S3 are more general. Our approach is similar to, but generalizes, the results in Andrieu and Roberts [2009] and Andrieu and Vihola [2015] to more complex sampling schemes.*

To develop the theory of Sampling Schemes S2 and S3 we require the following definitions. Let $\{V^{(n)}, n = 1, 2, \dots\}$ be the iterates of a Markov chain defined on the state space $\mathcal{V} := \mathcal{U} \times \mathbb{N} \times \Theta$. For $i = 1, \dots, p$, let $K_i(v; \cdot)$ be the substochastic transition kernel of the i th step of Sampling Scheme S2 that defines the probabilities for accepted Metropolis-Hastings moves and define

$$K := K_1 K_2 \dots K_p$$

to be the substochastic transition kernel that defines the probabilities for accepted Metropolis-Hastings moves. Note that probabilities involving the substochastic kernels provide lower bounds on the probabilities for the transition kernel of the corresponding Markov chain.

For $i = 1, \dots, p_1$

$$K_i(U_{1:T}, J, \theta_{-i}, \theta_i; U_{1:T}^*, J_i^*, \theta_{-i}, \theta_i^*) = \tilde{\pi}^N(J^*|U_{1:T}^*, \theta_{-i}, \theta_i^*) q_i(U_{1:T}^*, \theta_i^*|U_{1:T}, J, \theta_{-i}, \theta_i) \times \alpha_i(U_{1:T}, J, \theta_i; U_{1:T}^*, J^*, \theta_i^*|\theta_{-i}).$$

Similarly, for $i = 1, \dots, p$, let $\tilde{K}_i(v; \cdot)$ be the substochastic transition kernel of the i th step of Sampling Scheme S3 that defines the probabilities for accepted Metropolis-Hastings moves and define

$$\tilde{K} = \tilde{K}_1 \tilde{K}_2 \dots \tilde{K}_p,$$

where the kernels K_i and \tilde{K}_i only differ for $i = 1, \dots, p_1$.

The next theorem gives a sufficient condition for Sampling Scheme S2 to be irreducible and aperiodic and is similar to Theorem 1 of Andrieu and Roberts [2009].

Theorem S1 *If \tilde{K} is irreducible and aperiodic then K is irreducible and aperiodic. **Proof.** For $i = 1, \dots, p_1$, $\tilde{\pi}^N(\cdot|\theta_{-i}, \theta_i^*) \ll \psi(\cdot|\theta_{-i}, \theta_i^*)$ and the result now follows from Assumption 1 of Andrieu et al. [2010]. ■*

We now follow the approach in Andrieu and Roberts [2009] and show the uniform ergodicity of the sampling schemes by giving sufficient conditions for the existence of minorization conditions for Sampling Scheme S2. These minorization conditions are equivalent to uniform ergodicity by Theorem 8 of Roberts and Rosenthal [2004]. The results use the following technical lemmas.

Lemma S2 *For $i = 1, \dots, p_1$,*

$$\alpha_i(U_{1:T}, J, \theta_i; U_{1:T}^*, J^*, \theta_i^*|\theta_{-i}) \geq \left\{ 1 \wedge \frac{\tilde{\pi}^N(U_{1:T}^*|\theta_{-i}, \theta_i^*) \psi(U_{1:T}|\theta_{-i}, \theta_i)}{\tilde{\pi}^N(U_{1:T}|\theta_{-i}, \theta_i) \psi(U_{1:T}^*|\theta_{-i}, \theta_i^*)} \right\} \times \tilde{\alpha}_i(U_{1:T}, J, \theta_i; U_{1:T}^*, J^*, \theta_i^*|\theta_{-i})$$

Proof. From (S1),

$$\begin{aligned} & \alpha_i(U_{1:T}, J, \theta_i; U_{1:T}^*, J^*, \theta_i^*|\theta_{-i}) \\ &= 1 \wedge \frac{\tilde{\pi}^N(U_{1:T}^*, \theta_i^*|\theta_{-i}) q_i(U_{1:T}, \theta_i|U_{1:T}^*, J^*, \theta_{-i}, \theta_i^*)}{\tilde{\pi}^N(U_{1:T}, \theta_i|\theta_{-i}) q_i(U_{1:T}^*, \theta_i^*|U_{1:T}, J, \theta_{-i}, \theta_i)} \\ &= 1 \wedge \frac{\tilde{\pi}^N(U_{1:T}^*|\theta_{-i}, \theta_i^*) \psi(U_{1:T}|\theta_{-i}, \theta_i)}{\tilde{\pi}^N(U_{1:T}|\theta_{-i}, \theta_i) \psi(U_{1:T}^*|\theta_{-i}, \theta_i^*)} \times \frac{\tilde{\pi}^N(\theta_i^*|\theta_{-i}) q_{i,1}(\theta_i|U_{1:T}^*, J^*, \theta_{-i}, \theta_i^*)}{\tilde{\pi}^N(\theta_i|\theta_{-i}) q_{i,1}(\theta_i^*|U_{1:T}, J, \theta_{-i}, \theta_i)} \\ &\geq 1 \wedge \frac{\tilde{\pi}^N(U_{1:T}^*|\theta_{-i}, \theta_i^*) \psi(U_{1:T}|\theta_{-i}, \theta_i)}{\tilde{\pi}^N(U_{1:T}|\theta_{-i}, \theta_i) \psi(U_{1:T}^*|\theta_{-i}, \theta_i^*)} \times 1 \wedge \frac{\tilde{\pi}^N(\theta_i^*|\theta_{-i}) q_{i,1}(\theta_i|U_{1:T}^*, J^*, \theta_{-i}, \theta_i^*)}{\tilde{\pi}^N(\theta_i|\theta_{-i}) q_{i,1}(\theta_i^*|U_{1:T}, J, \theta_{-i}, \theta_i)} \\ &= \left\{ 1 \wedge \frac{\tilde{\pi}^N(U_{1:T}^*|\theta_{-i}, \theta_i^*) \psi(U_{1:T}|\theta_{-i}, \theta_i)}{\tilde{\pi}^N(U_{1:T}|\theta_{-i}, \theta_i) \psi(U_{1:T}^*|\theta_{-i}, \theta_i^*)} \right\} \times \tilde{\alpha}_i(U_{1:T}, J, \theta_i; U_{1:T}^*, J^*, \theta_i^*|\theta_{-i}) \end{aligned}$$

■

Lemma S3 *Suppose that*

$$\frac{\tilde{\pi}^N(U_{1:T}^*|\theta)}{\psi(U_{1:T}^*|\theta)} \leq \gamma < \infty \quad (\text{S5})$$

for all $U_{1:T}^* \in \mathcal{U}, \theta \in \mathcal{S}$. Then, for $i = 1, \dots, p_1$, each Markov transition kernel K_i satisfies

$$K_i \geq \gamma^{-1} \tilde{K}_i \quad (\text{S6})$$

and hence

$$K \geq \gamma^{-p_1} \tilde{K}. \quad (\text{S7})$$

Proof. Fix $i \in \{1, \dots, p_1\}$ and let $A \in \mathcal{B}(\mathcal{U})$, $J, J^* \in \{1, \dots, N\}$ and $B \in \mathcal{B}(\Theta_i)$. Then

$$\begin{aligned} & K_i(U_{1:T}, J, \theta_{-i}, \theta_i; A, J^*, \theta_{-i}, B) \\ &= \int_{A \times B} \tilde{\pi}^N(J^*|U_{1:T}^*, \theta_{-i}, \theta_i^*) q_i(U_{1:T}^*, \theta_i^*|U_{1:T}, J, \theta_{-i}, \theta_i) \times \\ & \quad \alpha_i(U_{1:T}, J, \theta_i; U_{1:T}^*, J^*, \theta_i^*|\theta_{-i}) dU_{1:T}^* d\theta_i^* \\ &\geq \int_{A \times B} \tilde{\pi}^N(J^*|U_{1:T}^*, \theta_{-i}, \theta_i^*) q_i(U_{1:T}^*, \theta_i^*|U_{1:T}, J, \theta_{-i}, \theta_i) \times \\ & \quad \left\{ 1 \wedge \frac{\tilde{\pi}^N(U_{1:T}^*|\theta_{-i}, \theta_i^*) \psi(U_{1:T}|\theta_{-i}, \theta_i)}{\tilde{\pi}^N(U_{1:T}|\theta_{-i}, \theta_i) \psi(U_{1:T}^*|\theta_{-i}, \theta_i^*)} \right\} \times \tilde{\alpha}_i(U_{1:T}, J, \theta_i; U_{1:T}^*, J^*, \theta_i^*|\theta_{-i}) dU_{1:T}^* d\theta_i^* \\ &\geq \gamma^{-1} \int_{A \times B} \tilde{\pi}^N(U_{1:T}^*, J^*|\theta_{-i}, \theta_i^*) q_{i,1}(\theta_i^*|U_{1:T}, J, \theta_{-i}, \theta_i) \times \tilde{\alpha}_i(U_{1:T}, J, \theta_i; U_{1:T}^*, J^*, \theta_i^*|\theta_{-i}) dU_{1:T}^* d\theta_i^* \\ &= \gamma^{-1} \tilde{K}_i(U_{1:T}, J, \theta_{-i}, \theta_i; A, J^*, \theta_{-i}, B), \end{aligned}$$

which proves (S6). Apply (S6) for each i to get (S7) ■ Lemma S3 can be used to find sufficient conditions for the existence of minorization conditions for Sampling Scheme S2 as given in the theorem below, which is similar to Andrieu and Roberts [2009], Theorem 8. Let $\mathcal{L}_N\{V^{(n)} \in \cdot\}$ denote the sequence of distribution functions of the random variables $\{V^{(n)} : n = 1, 2, \dots\}$, generated by Sampling Scheme S2, and let $|\cdot|_{TV}$ be total variation norm.

Theorem S4 *Suppose that Sampling Scheme S3 satisfies the following minorization condition: there exists a constant $\epsilon > 0$, a number $n_0 \geq 1$, and a probability measure ν on \mathcal{V} such that $\tilde{K}^{n_0}(v; A) \geq \epsilon \nu(A)$ for all $v \in \mathcal{V}, A \in \mathcal{B}(\mathcal{V})$. Suppose also that the conditions of Lemma S3 are satisfied. Then Sampling Scheme S2 satisfies the minorization condition*

$$K^{n_0}(v; A) \geq \gamma^{-p_1 n_0} \epsilon \nu(A)$$

and for all starting values for the Markov Chain

$$|\mathcal{L}_N\{V^{(n)} \in \cdot\} - \tilde{\pi}^N\{V^{(n)} \in \cdot\}|_{TV} \leq (1 - \delta)^{\lfloor n/n_0 \rfloor},$$

where $0 < \delta < 1$ and $\lfloor n/n_0 \rfloor$ is the greatest integer not exceeding n/n_0 .

Proof. To show the first part, suppose $\tilde{K}^{n_0}(v; A) \geq \epsilon \nu(A)$ for all $v \in \mathcal{V}, A \in \mathcal{B}(\mathcal{V})$. Fix $v \in \mathcal{V}, A \in \mathcal{B}(\mathcal{V})$. Applying Lemma S3 repeatedly gives

$$K^{n_0}(v; A) \geq \gamma^{-p_1 n_0} \tilde{K}^{n_0}(v; A) \geq \gamma^{-p_1 n_0} \epsilon \nu(A)$$

as required. The second part follows from the first part and Roberts and Rosenthal [2004], Theorem 8. ■

Lemma S5 gives sufficient conditions for Lemma S3 to hold. The first condition is from Andrieu et al. [2010].

Lemma S5 *Suppose*

- (i) *There is a sequence of finite, positive constants $\{c_t : t = 1, \dots, T\}$ such that for any $x_{1:t} \in \mathcal{S}_t(\theta)$ and all $\theta \in \mathcal{S}$, $f_\theta(x_t|x_{t-1})g_\theta(y_t|x_t) \leq c_t m_t^\theta(x_t|x_{t-1})$.*
- (ii) *There exists an $\epsilon > 0$ such that for all $\theta \in \mathcal{S}$, $p(y_{1:T}|\theta) > \epsilon$.*

If (i) and (ii) hold, then the conditions in Lemma S3 are satisfied.

Proof. Part (i) implies that for all $\theta \in \mathcal{S}$ and all $U_{1:T} \in \mathcal{U}$, $Z(U_{1:T}, \theta) \leq \prod_{t=1}^T c_t$. Hence Part (ii) implies that

$$\frac{Z(U_{1:T}, \theta)}{p(y_{1:T}|\theta)} < \frac{\prod_{t=1}^T c_t}{\epsilon}.$$

From (7),

$$\frac{\tilde{\pi}^N(U_{1:T}^*|\theta)}{\psi(U_{1:T}^*|\theta)} = \frac{Z(U_{1:T}, \theta)}{p(y_{1:T}|\theta)}$$

giving the result. ■

Remark S4 *The results above can be modified for the factor stochastic volatility model given in Section 4 in a straightforward way. Details are available from the authors on request.*

Remark S5 *If the states are sampled using backward simulation, similar arguments can be applied to obtain corresponding results (see Section S3). The mathematical details of the derivation use the results in Olsson and Ryden [2011] and Lindsten and Schön [2012a].*

S3 Backward simulation

Godsill et al. [2004] introduce the *backward simulation* algorithm which samples the indices J_T, J_{T-1}, \dots, J_1 sequentially, and differs from *ancestral tracing* which samples one index J and traces back its ancestral lineage. The *backward simulation* algorithm (Algorithm S3 below) is used in the PMCMC setting by Olsson and Ryden [2011] (in the PMMH algorithm)

and Lindsten and Schön [2012a] (in the PG algorithm). Chopin and Singh [2015] studied the PG algorithm with *backward simulation* and found that it yields a smaller autocorrelation than the corresponding algorithm using *ancestral tracing*. Moreover, it is more robust to the resampling scheme (multinomial resampling, systematic resampling, residual resampling or stratified resampling) used in the resampling step of the algorithm.

Algorithm S3 (Backward Simulation) 1. Sample $J_T = j_t$ conditional on $u_{1:T}$, with probability proportional to $w_T^{j_T}$, and choose $x_T^{j_T}$;

2. For $t = T - 1, \dots, 1$, sample $J_t = j_t$ conditional on

$$(u_{1:t}, j_{t+1:T}, x_{t+1}^{j_{t+1}}, \dots, x_T^{j_T}),$$

with probability proportional to $w_t^{j_t} f_\theta(x_{t+1}^{j_{t+1}} | x_t^{j_t})$, and choose $x_t^{j_t}$.

We denote the particles selected and the trajectory selected by $x_{1:T}^{j_{1:T}} = (x_1^{j_1}, \dots, x_T^{j_T})$ and $j_{1:T}$, respectively. With some abuse of notation, we denote

$$x_{1:T}^{(-j_{1:T})} = \left\{ x_1^{(-j_1)}, \dots, x_T^{(-j_T)} \right\}.$$

It will simplify the notation to sometimes use the following one-to-one transformation

$$(u_{1:T}, j_{1:T}) \leftrightarrow \left\{ x_{1:T}^{j_{1:T}}, j_{1:T}, x_{1:T}^{(-j_{1:T})}, a_{1:T-1} \right\},$$

and switch between the two representations and use whichever is more convenient.

The augmented space in this case consists of the particle filter variables $U_{1:T}$ and the sampled trajectory $J_{1:T}$ and PMCMC methods using *backward simulation* target the following density

$$\begin{aligned} \tilde{\pi}_{BSi}^N \left(x_{1:T}, j_{1:T}, x_{1:T}^{(-j_{1:T})}, a_{1:T-1}, \theta \right) &:= \\ &\frac{p(x_{1:T}, \theta | y_{1:T})}{N^T} \frac{\psi(u_{1:T} | \theta)}{m_1^\theta(x_1^{b_1}) \prod_{t=2}^T \bar{w}_{t-1}^{a_{t-1}^i} m_t^\theta \left(x_t^{b_t} | x_{t-1}^{a_{t-1}^{b_t}} \right)} \times \\ &\prod_{t=2}^T \frac{w_t^{a_{t-1}^{j_t}} f(x_t^{j_t} | x_{t-1}^{a_{t-1}^{j_t}})}{\sum_{i=1}^N w_t^{a_{t-1}^i} f(x_t^i | x_{t-1}^{a_{t-1}^i})}. \end{aligned} \quad (\text{S8})$$

Olsson and Ryden [2011] show that, under Assumption 2 of Andrieu et al. [2010],

$$\tilde{\pi}_{BSi}^N \left(x_{1:T}, j_{1:T}, x_{1:T}^{(-j_{1:T})}, a_{1:T-1}, \theta \right)$$

has the following marginal distribution

$$\tilde{\pi}_{BSi}^N(x_{1:T}, j_{1:T}, \theta) = \frac{p(x_{1:T}, \theta | y_{1:T})}{N^T},$$

and hence

$$\tilde{\pi}_{BSi}^N(x_{1:T}, \theta) = p(x_{1:T}, \theta | y_{1:T}).$$

The conditional sequential Monte Carlo algorithm used in the backward simulation also changes. It is given in Lindsten et al. [2014] and generates from the full conditional distribution

$$\tilde{\pi}_{BSi}^N \left(x_{1:T}^{(-j_{1:T})}, a_{1:T-1} | x_{1:T}, j_{1:T}, \theta \right).$$

The general sampler using *backward simulation* is analogous to the *ancestral tracing* general sampler, but on an expanded space.

Sampling Scheme S4 (general-BSi) *Given initial values for $U_{1:T}$, $J_{1:T}$ and θ , one iteration of the MCMC involves the following steps*

1. (PMMH sampling) For $i = 1, \dots, p_1$

Step i :

- (a) Sample $\theta_i^* \sim q_{BSi,i,1}(\cdot | U_{1:T}, J_{1:T}, \theta_{-i}, \theta_i)$.
- (b) Sample $U_{1:T}^* \sim \psi(\cdot | \theta_{-i}, \theta_i^*)$.
- (c) Sample $J_{1:T}^*$ from $\tilde{\pi}_{BSi}^N(\cdot | U_{1:T}^*, \theta_{-i}, \theta_i^*)$.
- (d) Set $(\theta_i, U_{1:T}, J_{1:T}) \leftarrow (\theta_i^*, U_{1:T}^*, J_{1:T}^*)$ with probability

$$\begin{aligned} \alpha_i(U_{1:T}, J_{1:T}, \theta_i; U_{1:T}^*, J_{1:T}^*, \theta_i^* | \theta_{-i}) &= \\ 1 \wedge \frac{\tilde{\pi}_{BSi}^N(U_{1:T}^*, \theta_i^* | \theta_{-i})}{\tilde{\pi}_{BSi}^N(U_{1:T}, \theta_i | \theta_{-i})} \frac{q_{BSi,i}(U_{1:T}, \theta_i | U_{1:T}^*, J_{1:T}^*, \theta_{-i}, \theta_i^*)}{q_{BSi,i}(U_{1:T}^*, \theta_i^* | U_{1:T}, J_{1:T}, \theta_{-i}, \theta_i)} & \quad (\text{S9}) \end{aligned}$$

where

$$q_{BSi,i}(U_{1:T}^*, \theta_i^* | U_{1:T}, J_{1:T}, \theta_{-i}, \theta_i) = q_{BSi,i,1}(\theta_i^* | U_{1:T}, J_{1:T}, \theta_{-i}, \theta_i) \psi(U_{1:T}^* | \theta_{-i}, \theta_i^*).$$

2. (PG or PMwG sampling) For $i = p_1 + 1, \dots, p$

Step i :

- (a) Sample $\theta_i^* \sim q_i(\cdot | X_{1:T}^J, B_{1:T-1}^J, J, \theta_{-i}, \theta_i)$.
- (b) Set $\theta_i \leftarrow \theta_i^*$ with probability

$$\begin{aligned} \alpha_i(\theta_i; \theta_i^* | X_{1:T}^J, B_{1:T-1}^J, J, \theta_{-i}) &= \\ = 1 \wedge \frac{\tilde{\pi}^N(\theta_i^* | X_{1:T}^J, B_{1:T-1}^J, J, \theta_{-i})}{\tilde{\pi}^N(\theta_i | X_{1:T}^J, B_{1:T-1}^J, J, \theta_{-i})} \frac{q_i(\theta_i | X_{1:T}^J, B_{1:T-1}^J, J, \theta_{-i}, \theta_i^*)}{q_i(\theta_i^* | X_{1:T}^J, B_{1:T-1}^J, J, \theta_{-i}, \theta_i)}. & \end{aligned}$$

3. Sample $U_{1:T}^{(-J),*} \sim \tilde{\pi}^N(\cdot | X_{1:T}^J, B_{1:T-1}^J, J, \theta_{-i}, \theta_i^*)$.

4. Sample $J \sim \tilde{\pi}^N(\cdot | U_{1:T}, \theta)$

The PMMH steps in Sampling Scheme S4 simplify similarly to Sampling Scheme S2. Olsson and Ryden [2011] show that

$$\frac{\tilde{\pi}_{BSi}^N(U_{1:T}, \theta_i | \theta_{-i})}{\psi(U_{1:T} | \theta_{-i}, \theta_i)} = \frac{Z(U_{1:T}, \theta) p(\theta_i | \theta_{-i})}{p(y_{1:T} | \theta_{-i})},$$

which is the same expression as (7). Hence, the Metropolis-Hastings acceptance probability in (S9) simplifies to

$$1 \wedge \frac{Z(\theta_i^*, \theta_{-i}, U_{1:T}^*)}{Z(\theta_i, \theta_{-i}, U_{1:T})} \frac{q_{BSi,i,1}(\theta_i | U_{1:T}^*, J^*, \theta_{-i}, \theta_i^*) p(\theta_i^* | \theta_{-i})}{q_{BSi,i,1}(\theta_i^* | U_{1:T}, J, \theta_{-i}, \theta_i) p(\theta_i | \theta_{-i})}.$$

The results in Section S2 can be modified for the distribution $\tilde{\pi}_{BSi}^N(\cdot)$, instead of the distribution $\tilde{\pi}^N(\cdot)$ in a straightforward way. Details are available from the authors on request.

S4 Target density for the factor SV model

This section discusses the target density of the PMMH+PG sampler for the multivariate factor SV model outlined in Section 4.1. Section S4.1 discusses an appropriate target density for the closed form density case and Section S4.2 discusses an appropriate target density for a factor SV model with the Euler approximation.

S4.1 The closed form density case

This section provides an appropriate target density for a factor SV model with the closed form state transition density given in equation (19). The target density includes all the random variables produced by $K + S$ univariate particle filters that generate the factor log volatilities $\boldsymbol{\lambda}_{k,1:T}$ for $k = 1, \dots, K$ and the idiosyncratic log volatilities $\boldsymbol{h}_{s,1:T}$ for $s = 1, \dots, S$, as well as the factors $\boldsymbol{f}_{1:T}$ and the parameters $\boldsymbol{\omega}$. It is convenient in the developments below to define $\boldsymbol{\theta} = (\boldsymbol{f}_{1:T}, \boldsymbol{\omega})$.

To specify the univariate particle filters that generate the factor log volatilities $\boldsymbol{\lambda}_{k,1:T}$ for $k = 1, \dots, K$, we use equations (17) and (23) and to generate the idiosyncratic log volatilities $\boldsymbol{h}_{s,1:T}$, for $s = 1, \dots, S$, we use equations (19) and (24). We denote the weighted samples by $(\boldsymbol{\lambda}_{k,t}^{1:N}, \bar{w}_{f,k,t}^{1:N})$ and $(\boldsymbol{h}_{s,t}^{1:N}, \bar{w}_{\epsilon,s,t}^{1:N})$. We denote the proposal densities by $m_{f,k,1}^{\boldsymbol{\theta}}(\lambda_{k,1})$, $m_{f,k,t}^{\boldsymbol{\theta}}(\lambda_{k,t} | \lambda_{k,t-1})$, $m_{\epsilon,s,1}^{\boldsymbol{\theta}}(h_{s,1})$ and $m_{\epsilon,s,t}^{\boldsymbol{\theta}}(h_{s,t} | h_{s,t-1})$ for $t = 2, \dots, T$. We denote the resampling schemes by $\mathcal{M}_f(\boldsymbol{a}_{f,k,t-1}^{1:N} | \bar{w}_{f,k,t-1}^{1:N})$ for $k = 1, \dots, K$, where each $a_{f,k,t-1}^i = j$ indexes a particle in $(\boldsymbol{\lambda}_{k,t}^{1:N}, \bar{w}_{f,k,t}^{1:N})$ and is chosen with probability $\bar{w}_{f,k,t}^j$; the resampling scheme $\mathcal{M}_\epsilon(\boldsymbol{a}_{\epsilon,s,t-1}^{1:N} | \bar{w}_{\epsilon,s,t-1}^{1:N})$ for $s = 1, \dots, S$ is defined similarly. We denote the vector of particles by

$$\boldsymbol{U}_{f,1:K,1:T} = (\boldsymbol{\lambda}_{1:K,1:T}^{1:N}, \boldsymbol{A}_{f,1:K,1:T-1}^{1:N}), \quad (\text{S10})$$

and

$$\boldsymbol{U}_{\epsilon,1:S,1:T} = (\boldsymbol{h}_{1:S,1:T}^{1:N}, \boldsymbol{A}_{\epsilon,1:S,1:T-1}^{1:N}). \quad (\text{S11})$$

The joint distribution of the particles given the parameters is

$$\psi_{f,k}(\mathbf{U}_{f,k,1:T}|\boldsymbol{\theta}) = \prod_{i=1}^N m_{f,k,1}^{\boldsymbol{\theta}}(\lambda_{k,1}^i) \prod_{t=2}^T \left\{ \mathcal{M}_f(\mathbf{a}_{f,k,t-1}^{1:N} | \bar{w}_{f,k,t-1}^{1:N}) \prod_{i=1}^N m_{f,k,t}^{\boldsymbol{\theta}}(\lambda_{f,k,t}^i | \lambda_{f,k,t-1}^{a_{f,k,t-1}^i}) \right\}, \quad (\text{S12})$$

for $k = 1, \dots, K$, and

$$\psi_{\epsilon,s}(\mathbf{U}_{\epsilon,s,1:T}|\boldsymbol{\theta}) = \prod_{i=1}^N m_{\epsilon,s,1}^{\boldsymbol{\theta}}(h_{s,1}^i) \prod_{t=2}^T \left\{ \mathcal{M}_{\epsilon}(\mathbf{a}_{\epsilon,s,t-1}^{1:N} | \bar{w}_{\epsilon,s,t-1}^{1:N}) \prod_{i=1}^N m_{\epsilon,s,t}^{\boldsymbol{\theta}}(h_{s,t}^i | h_{s,t-1}^{a_{\epsilon,s,t-1}^i}) \right\}, \quad (\text{S13})$$

for $s = 1, \dots, S$.

Next, we define indices $J_{f,k} = j$ for each $k = 1, \dots, K$, then trace back its ancestral lineage $b_{f,k,1:T}^j$ ($b_{f,k,T}^j = j, b_{f,k,t-1}^j = a_{f,k,t-1}^{b_{f,k,t}^j}$), and select the particle trajectory $\boldsymbol{\lambda}_{k,1:T}^j = (\lambda_{k,1}^{b_{f,k,1}^j}, \dots, \lambda_{k,T}^{b_{f,k,T}^j})$. Similarly, we define indices $J_{\epsilon,s} = j$ for each $s = 1, \dots, S$, then trace back its ancestral lineage $b_{\epsilon,s,1:T}^j$ ($b_{\epsilon,s,T}^j = j, b_{\epsilon,s,t-1}^j = a_{\epsilon,s,t-1}^{b_{\epsilon,s,t}^j}$), and select the particle trajectory $\mathbf{h}_{s,1:T}^j = (h_{s,1}^{b_{\epsilon,s,1}^j}, \dots, h_{s,T}^{b_{\epsilon,s,T}^j})$.

The augmented target density of the factor model is defined as

$$\begin{aligned} \tilde{\pi}^N(\mathbf{U}_{f,1:K,1:T}, \mathbf{U}_{\epsilon,1:S,1:T}, \mathbf{J}_f, \mathbf{J}_{\epsilon}, \boldsymbol{\theta}) := \\ \frac{\pi(\boldsymbol{\lambda}_{1:K,1:T}^{\mathbf{J}_f}, \mathbf{h}_{1:S,1:T}^{\mathbf{J}_{\epsilon}}, \boldsymbol{\theta})}{N^{T(K+S)}} \prod_{k=1}^K \frac{\psi_{f,k}(\mathbf{U}_{f,k,1:T}|\boldsymbol{\theta})}{m_{f,k,1}^{\boldsymbol{\theta}}(\lambda_{k,1}^{b_{f,k,1}^j}) \prod_{t=2}^T \bar{w}_{f,k,t-1}^{b_{f,k,t}^j} m_{f,k,t}^{\boldsymbol{\theta}}(\lambda_{k,t}^{b_{f,k,t}^j} | \lambda_{k,t-1}^{a_{f,k,t-1}^{b_{f,k,t}^j}})} \\ \prod_{s=1}^S \frac{\psi_{\epsilon,s}(\mathbf{U}_{\epsilon,s,1:T}|\boldsymbol{\theta})}{m_{\epsilon,s,1}^{\boldsymbol{\theta}}(h_{s,1}^{b_{\epsilon,s,1}^j}) \prod_{t=2}^T \bar{w}_{\epsilon,s,t-1}^{b_{\epsilon,s,t}^j} m_{\epsilon,s,t}^{\boldsymbol{\theta}}(h_{s,t}^{b_{\epsilon,s,t}^j} | h_{s,t-1}^{a_{\epsilon,s,t-1}^{b_{\epsilon,s,t}^j}})}. \end{aligned} \quad (\text{S14})$$

S4.2 Approximating the transition density by an Euler scheme

This section provides an appropriate target density for a factor model with the Euler approximation given in Eq. (20) or Eq. (22). We follow the approach in Lindsten et al. [2015] and introduce state vectors for $s = 1, \dots, S$ defined as $x_{s,1} = h_{s,1}$ and $x_{s,t} = (h_{s,t}, h_{s,t-1,M-1}, \dots, h_{s,t-1,1})^T$, for $t = 2, \dots, T$. The state transition densities are given by

$$f_{s,t}^{\theta}(x_{s,t}|x_{s,t-1}) = \prod_{j=1}^M f_{s,t-1,j}^{\theta}(h_{s,t-1,j} | h_{s,t-1,j-1}) \quad (t = 2, \dots, T), \quad (\text{S15})$$

where the densities $f_{s,t,j}^\theta(h_{s,t,j}|h_{s,t,j-1})$ for $j = 1, \dots, M$, $t = 1, \dots, T-1$ and $s = 1, \dots, S$ are defined by equation (20) or equation (22). We use the proposal densities

$$m_{\epsilon,s,t}^\theta(x_{s,t}|x_{s,t-1}) = f_{s,t}^\theta(x_{s,t}|x_{s,t-1}) \quad (t = 2, \dots, T \text{ and } s = 1, \dots, S)$$

which can be generated using equation (20) or equation (22). With these modifications, we use the same construction as Section S4.1. The modifications give

$$\mathbf{U}_{\epsilon,1:S,1:T} = (\mathbf{x}_{1:S,1:T}^{1:N}, \mathbf{A}_{\epsilon,1:S,1:T-1}^{1:N}) \quad (\text{S16})$$

$$\psi_{\epsilon,s}(\mathbf{U}_{\epsilon,s,1:T}|\boldsymbol{\theta}) = \prod_{i=1}^N m_{\epsilon,s,1}^\theta(x_{s,1}^i) \prod_{t=2}^T \left\{ \mathcal{M}_\epsilon(\mathbf{a}_{\epsilon,s,t-1}^{1:N} | \bar{w}_{\epsilon,s,t-1}^{1:N}) \prod_{i=1}^N m_{\epsilon,s,t}^\theta(x_{s,t}^i | x_{s,t-1}^{a_{\epsilon,s,t-1}^i}) \right\} \quad (\text{S17})$$

$$\begin{aligned} \tilde{\pi}^N(\mathbf{U}_{f,1:K,1:T}, \mathbf{U}_{\epsilon,1:S,1:T}, \mathbf{J}_f, \mathbf{J}_\epsilon, \boldsymbol{\theta}) := \\ \frac{\pi(\boldsymbol{\lambda}_{1:K,1:T}^{\mathbf{J}_f}, \mathbf{x}_{1:S,1:T}^{\mathbf{J}_\epsilon}, \boldsymbol{\theta})}{N^{T(K+S)}} \prod_{k=1}^K \frac{\psi_{f,k}(\mathbf{U}_{f,k,1:T}|\boldsymbol{\theta})}{m_{f,k,1}^\theta(\lambda_{k,1}^{b_{f,k,1}}) \prod_{t=2}^T \bar{w}_{f,k,t-1}^{a_{f,k,t-1}^{b_{f,k,t}}} m_{f,k,t}^\theta(\lambda_{k,t}^{b_{f,k,t}} | \lambda_{k,t-1}^{a_{f,k,t-1}^{b_{f,k,t}}})} \\ \prod_{s=1}^S \frac{\psi_{\epsilon,s}(\mathbf{U}_{\epsilon,s,1:T}|\boldsymbol{\theta})}{m_{\epsilon,s,1}^\theta(x_{s,1}^{b_{\epsilon,s,1}}) \prod_{t=2}^T \bar{w}_{\epsilon,s,t-1}^{a_{\epsilon,s,t-1}^{b_{\epsilon,s,t}}} m_{\epsilon,s,t}^\theta(x_{s,t}^{b_{\epsilon,s,t}} | x_{s,t-1}^{a_{\epsilon,s,t-1}^{b_{\epsilon,s,t}}})} \end{aligned} \quad (\text{S18})$$

S5 PMMH+PG sampling scheme for the factor SV model

Similarly to Section 3.3, we use the following notation to describe the algorithms used in the examples. The basic samplers, as used in Sampling Schemes 1 or S5, are PMMH(\cdot) and PG(\cdot). These samplers can be used alone or in combination. For example, PMMH($\boldsymbol{\theta}$) means using a PMMH step to sample the parameter vector $\boldsymbol{\theta}$; PMMH(θ_1) + PG(θ_2) means sampling θ_1 in the PMMH step and θ_2 in the PG step; and PG($\boldsymbol{\theta}$) means sampling $\boldsymbol{\theta}$ using the PG sampler.

We illustrate our methods using the $PMMH(\boldsymbol{\alpha}, \boldsymbol{\tau}_f^2, \boldsymbol{\tau}_\epsilon^2) + PG(\boldsymbol{\beta}, \mathbf{f}_{1:T}, \boldsymbol{\phi}, \boldsymbol{\mu})$ sampler, which we found to give good performance in the empirical studies in Section 4.2. It is straightforward to modify the sampling scheme for other choices of which parameters to sample with a PMMH step and which to sample with a PG step. Our procedure to determine an efficient sampling scheme is to run the PG algorithm first to identify which parameters have large IACT, or, in some cases, require a large amount of computational time to generate in the PG step. We then generate these parameters in the PMMH step. See, for example, our discussion of the univariate OU model in Section 3.3. In particular, we note that if an Euler approximation is used, then generating any parameter in the OU or GARCH model is

very time intensive as it is necessary to determine, store and use the ancestor history of the entire state vector.

The sampling schemes for the factor SV model with the closed form transition density given by equation (19) and the model with the Euler scheme given by equation (20) or equation (22) have the same structure, so Sampling Scheme S5 is given below in a generic form and the appropriate state space models are used for the different cases; see Sections S4.1 and S4.2 for details. We have simplified the conditional distributions in Sampling Scheme S5 wherever possible using the conditional independence properties discussed in Section 4.1. The Metropolis-Hastings proposal densities for Sampling scheme S5 are given in Section S5.1. We use the notation $\theta_{-i} := (\theta_1, \dots, \theta_{i-1}, \theta_{i+1}, \dots, \theta_p)$, where p is the total number of parameters.

Sampling Scheme S5 ($PMMH(\boldsymbol{\alpha}, \boldsymbol{\tau}_f^2, \boldsymbol{\tau}_\epsilon^2) + PG(\boldsymbol{\beta}, \mathbf{f}_{1:T}, \boldsymbol{\phi}, \boldsymbol{\mu})$) Given initial values for $U_{f,1:T}, U_{\epsilon,1:T}, J_f, J_\epsilon$ and θ , one iteration of the MCMC involves the following steps.

1. (PMMH sampling),

(a) For $k = 1, \dots, K$

- i. Sample $(\tau_{f,k}^{2*}) \sim q_{\tau_{f,k}^2}(\cdot | \mathbf{U}_{f,k,1:T}, \tau_{f,k}^2, \boldsymbol{\theta}_{-\tau_{f,k}^2})$
- ii. Sample $\mathbf{U}_{f,k,1:T}^* \sim \psi_{f,k}(\cdot | \tau_{f,k}^{2*}, \boldsymbol{\theta}_{-\tau_{f,k}^2})$
- iii. Sample $J_{f,k}^*$ from $\tilde{\pi}^N(\cdot | \mathbf{U}_{f,k,1:T}^*, \tau_{f,k}^{2*}, \boldsymbol{\theta}_{-\tau_{f,k}^2})$
- iv. Set $(\tau_{f,k}^2, \mathbf{U}_{f,k,1:T}, J_{f,k}) \leftarrow (\tau_{f,k}^{2*}, \mathbf{U}_{f,k,1:T}^*, J_{f,k}^*)$ with probability

$$\alpha \left(\mathbf{U}_{f,k,1:T}, J_{f,k}, \tau_{f,k}^2; \mathbf{U}_{f,k,1:T}^*, J_{f,k}^*, \tau_{f,k}^{2*} | \boldsymbol{\theta}_{-\tau_{f,k}^2} \right) = 1 \wedge \frac{Z \left(\mathbf{U}_{f,k,1:T}^*, \tau_{f,k}^{2*}, \boldsymbol{\theta}_{-\tau_{f,k}^2} \right) p \left(\tau_{f,k}^{2*} \right)}{Z \left(\mathbf{U}_{f,k,1:T}, \tau_{f,k}^2, \boldsymbol{\theta}_{-\tau_{f,k}^2} \right) p \left(\tau_{f,k}^2 \right)} \times \frac{q_{\tau_{f,k}^2} \left(\tau_{f,k}^2 | \mathbf{U}_{f,k,1:T}^*, \tau_{f,k}^{2*}, \boldsymbol{\theta}_{-\tau_{f,k}^2} \right)}{q_{\tau_{f,k}^2} \left(\tau_{f,k}^{2*} | \mathbf{U}_{f,k,1:T}, \tau_{f,k}^2, \boldsymbol{\theta}_{-\tau_{f,k}^2} \right)}.$$

(b) For $s = 1, \dots, S$,

- i. Sample $(\alpha_s^*, \tau_{\epsilon,s}^{2*}) \sim q_{\alpha_s, \tau_{\epsilon,s}^2}(\cdot | \mathbf{U}_{\epsilon,s,1:T}, \alpha_s, \tau_{\epsilon,s}^2, \boldsymbol{\theta}_{-\alpha_s, \tau_{\epsilon,s}^2})$
- ii. Sample $\mathbf{U}_{\epsilon,s,1:T}^* \sim \psi_{\epsilon,s}(\cdot | \alpha_s^*, \tau_{\epsilon,s}^{2*}, \boldsymbol{\theta}_{-\alpha_s, \tau_{\epsilon,s}^2})$
- iii. Sample $J_{\epsilon,s}^*$ from $\tilde{\pi}^N(\cdot | \mathbf{U}_{\epsilon,s,1:T}^*, \alpha_s^*, \tau_{\epsilon,s}^{2*}, \boldsymbol{\theta}_{-\alpha_s, \tau_{\epsilon,s}^2})$
- iv. Set $(\alpha_s, \tau_{\epsilon,s}^2, \mathbf{U}_{\epsilon,s,1:T}, J_{\epsilon,s}) \leftarrow (\alpha_s^*, \tau_{\epsilon,s}^{2*}, \mathbf{U}_{\epsilon,s,1:T}^*, J_{\epsilon,s}^*)$ with probability

$$\alpha \left(\mathbf{U}_{\epsilon,s,1:T}, J_s, (\alpha_s, \tau_{\epsilon,s}^2); \mathbf{U}_{\epsilon,s,1:T}^*, J_{\epsilon,s}^*, (\alpha_s^*, \tau_{\epsilon,s}^{2*}) | \boldsymbol{\theta}_{-\alpha_s, \tau_{\epsilon,s}^2} \right) = 1 \wedge \frac{Z \left(\mathbf{U}_{\epsilon,s,1:T}^*, \alpha_s^*, \tau_{\epsilon,s}^{2*}, \boldsymbol{\theta}_{-\alpha_s, \tau_{\epsilon,s}^2} \right) p \left(\alpha_s^*, \tau_{\epsilon,s}^{2*} \right)}{Z \left(\mathbf{U}_{\epsilon,s,1:T}, \alpha_s, \tau_{\epsilon,s}^2, \boldsymbol{\theta}_{-\alpha_s, \tau_{\epsilon,s}^2} \right) p \left(\alpha_s, \tau_{\epsilon,s}^2 \right)} \times \frac{q_{\alpha_s, \tau_{\epsilon,s}^2} \left(\alpha_s, \tau_{\epsilon,s}^2 | \mathbf{U}_{\epsilon,s,1:T}^*, \alpha_s^*, \tau_{\epsilon,s}^{2*}, \boldsymbol{\theta}_{-\alpha_s, \tau_{\epsilon,s}^2} \right)}{q_{\alpha_s, \tau_{\epsilon,s}^2} \left(\alpha_s^*, \tau_{\epsilon,s}^{2*} | \mathbf{U}_{\epsilon,s,1:T}, \alpha_s, \tau_{\epsilon,s}^2, \boldsymbol{\theta}_{-\alpha_s, \tau_{\epsilon,s}^2} \right)}.$$

2. (PG sampling)

(a) Sample $\beta | \lambda_{1:T}^{J_f}, \mathbf{h}_{1:T}^{J_\epsilon}, \mathbf{B}_{f,1:T-1}^{J_f}, \mathbf{B}_{\epsilon,1:T-1}^{J_\epsilon}, \mathbf{J}_f, \mathbf{J}_\epsilon, \boldsymbol{\theta}_{-\beta}, \mathbf{y}_{1:T}$ using equation (S19) in Appendix S5.2.

(b) Redraw the diagonal elements of β through the deep interweaving procedure described in Appendix S5.3. This step is necessary to improve the mixing of the factor loading matrix β .

(c) Sample $\mathbf{f}_{1:T} | \lambda_{1:T}^{J_f}, \mathbf{h}_{1:T}^{J_\epsilon}, \mathbf{B}_{f,1:T-1}^{J_f}, \mathbf{B}_{\epsilon,1:T-1}^{J_\epsilon}, \mathbf{J}_f, \mathbf{J}_\epsilon, \boldsymbol{\theta}_{-\mathbf{f}_{1:T}}, \mathbf{y}_{1:T}$ using equation (S20) in Appendix S5.4.

(d) For $k = 1, \dots, K$

i. Sample ϕ_k^* from the proposal $q_{\phi_k}(\cdot | \lambda_{k,1:T}^{J_{f,k}}, \boldsymbol{\theta}_{-\phi_k})$ and set $\phi_k \leftarrow \phi_k^*$ with probability

$$1 \wedge \frac{\tilde{\pi}^N \left(\phi_k^* | \lambda_{k,1:T}^{J_{f,k}}, \mathbf{B}_{f,k,1:T-1}, J_{f,k}, \boldsymbol{\theta}_{-\phi_k} \right)}{\tilde{\pi}^N \left(\phi_k | \lambda_{k,1:T}^{J_{f,k}}, \mathbf{B}_{f,k,1:T-1}, J_{f,k}, \boldsymbol{\theta}_{-\phi_k} \right)} \times \frac{q_{\phi_k} \left(\phi_k | \lambda_{k,1:T}^{J_{f,k}}, \boldsymbol{\theta}_{-\phi_k} \right)}{q_{\phi_k} \left(\phi_k^* | \lambda_{k,1:T}^{J_{f,k}}, \boldsymbol{\theta}_{-\phi_k} \right)}.$$

ii. Sample $\mathbf{U}_{f,k,1:T}^{(-J_{f,k})} \sim \tilde{\pi}^N(\cdot | \lambda_{k,1:T}^{J_{f,k}}, \mathbf{B}_{f,k,1:T-1}, J_{f,k}, \boldsymbol{\theta})$ using the conditional sequential Monte Carlo algorithm (CSMC) discussed in Section S2.

iii. Sample $J_{f,k} \sim \tilde{\pi}^N(\cdot | \mathbf{U}_{f,k,1:T}, \boldsymbol{\theta})$.

(e) For $s = 1, \dots, S$,

i. Sample μ_s^* from the proposal $q_{\mu_s}(\cdot | \mathbf{h}_{s,1:T}^{J_{\epsilon,s}}, \boldsymbol{\theta}_{-\mu_s})$ and set $\mu_s \leftarrow \mu_s^*$ with probability

$$1 \wedge \frac{\tilde{\pi}^N \left(\mu_s^* | \mathbf{h}_{s,1:T}^{J_{\epsilon,s}}, \mathbf{B}_{\epsilon,s,1:T-1}, J_{\epsilon,s}, \boldsymbol{\theta}_{-\mu_s} \right)}{\tilde{\pi}^N \left(\mu_s | \mathbf{h}_{s,1:T}^{J_{\epsilon,s}}, \mathbf{B}_{\epsilon,s,1:T-1}, J_{\epsilon,s}, \boldsymbol{\theta}_{-\mu_s} \right)} \times \frac{q_{\mu_s} \left(\mu_s | \mathbf{h}_{s,1:T}^{J_{\epsilon,s}}, \boldsymbol{\theta}_{-\mu_s} \right)}{q_{\mu_s} \left(\mu_s^* | \mathbf{h}_{s,1:T}^{J_{\epsilon,s}}, \boldsymbol{\theta}_{-\mu_s} \right)}$$

ii. Sample $\mathbf{U}_{\epsilon,s,1:T}^{(-J_{\epsilon,s})} \sim \tilde{\pi}^N(\cdot | \mathbf{h}_{s,1:T}^{J_{\epsilon,s}}, \mathbf{B}_{\epsilon,s,1:T-1}, J_{\epsilon,s}, \boldsymbol{\theta})$ using the conditional sequential Monte Carlo algorithm (CSMC) discussed in Section 2.3.

iii. Sample $J_{\epsilon,s} \sim \tilde{\pi}^N(\cdot | \mathbf{U}_{\epsilon,s,1:T}, \boldsymbol{\theta})$.

S5.1 Proposal densities

This section details the proposal densities used in Sampling Scheme S5 for the exact OU model given by equation (19). We will specify other cases such as the Euler evolution given by equation (20) and the GARCH diffusion model given by equation (22) when describing the sampling scheme.

- For $k = 1, \dots, K$, $q_{\tau_{f,k}^2}$ is an adaptive random walk.

- For $s = 1, \dots, S$, $q_{\alpha_s, \tau_{\epsilon, s}^2}$ is an adaptive random walk.
- For $k = 1, \dots, K$, $q_{\phi_k}(\cdot | \boldsymbol{\lambda}_{k, 1:T}^{J_{f, k}}, \boldsymbol{\theta}_{-\phi_k}) = N(c_{\phi_k}, d_{\phi_k})$, where

$$c_{\phi_k} = \frac{d_{\phi_k}}{\tau_{f, k}^2} \sum_{t=2}^T \lambda_{k, t} \lambda_{k, t-1}, \quad \text{and} \quad d_{\phi_k} = \frac{\tau_{f, k}^2}{\sum_{t=2}^{T-1} \lambda_{k, t}^2},$$

- For $s = 1, \dots, S$, $q_{\mu_s}(\cdot | \mathbf{h}_{s, 1:T}^{J_{\epsilon, s}}, \boldsymbol{\theta}_{-\mu_s}) = N(c_{\mu_s}, d_{\mu_s})$, where

$$c_{\mu_s} = \frac{d_{\mu_s}}{\tau_{\epsilon, s}^2} \left(h_{s, 1} (2\alpha_s) + \left(\frac{2\alpha_s}{1 - \exp(-2\alpha_s)} \right) \left(\sum_{t=2}^T (h_{s, t} - \exp(-\alpha_s) h_{s, t} + \exp(-2\alpha_s) h_{s, t-1} - \exp(-\alpha_s) h_{s, t-1}) \right) \right),$$

$$d_{\mu_s} = \frac{\tau_{\epsilon, s}^2}{(2\alpha_s) + \left(\frac{2\alpha_s}{1 - \exp(-2\alpha_s)} \right) (T-1) (1 - 2\exp(-\alpha_s) + \exp(-2\alpha_s))^2},$$

S5.2 Sampling the factor loading matrix $\boldsymbol{\beta}$

First, to identify the parameters for the factor loading matrix $\boldsymbol{\beta}$, we follow the usual convention and set the upper triangular part of $\boldsymbol{\beta}$ to zero (Geweke and Zhou [1996]). This parameterisation imposes an order dependence. Second, the model is also not identified without further constraining either the scale of the k th column of $\boldsymbol{\beta}$ or the variance of $f_{k, t}$. The usual solution is to set the diagonal elements of the factor loading matrix $\boldsymbol{\beta}_{k, k}$ to one, for $k = 1, \dots, K$, while the level $\mu_{f, k}$ of the factor volatility $\lambda_{k, t}$ is modeled to be unknown. However, Kastner et al. [2017] note that this approach makes the variable ordering dependence stronger. We therefore follow Kastner et al. [2017] and leave the diagonal elements $\boldsymbol{\beta}_{k, k}$ unrestricted and set the level $\mu_{f, k}$ of the factor volatility $\lambda_{k, t}$ to zero for $k = 1, \dots, K$.

Let k_s denote the number of unrestricted elements in row s of $\boldsymbol{\beta}$ and define

$$\mathbf{F}_s = \begin{bmatrix} f_{1, 1} & \cdots & f_{k_s, 1} \\ \vdots & & \vdots \\ f_{1, T} & \cdots & f_{k_s, T} \end{bmatrix}, \quad \text{and} \quad \tilde{\mathbf{V}}_s = \begin{bmatrix} \exp(h_{s, 1}) & \cdots & 0 \\ 0 & \ddots & 0 \\ 0 & \cdots & \exp(h_{s, T}) \end{bmatrix}.$$

We sample the factor loadings $\boldsymbol{\beta}_{s, \cdot} = (\beta_{s, 1}, \dots, \beta_{s, k_s})^T$, for $s = 1, \dots, S$, independently for each s using the Gibbs-update

$$\boldsymbol{\beta}_{s, \cdot} | \mathbf{f}, \mathbf{y}_{s, \cdot}, \mathbf{h}_{s, \cdot} \sim N_{k_s}(a_{s, T}, b_{s, T}), \quad (\text{S19})$$

where $b_{s, T} = \left(\mathbf{F}_s^T \tilde{\mathbf{V}}_s^{-1} \mathbf{F}_s + I_{k_s} \right)^{-1}$ and $a_{s, T} = b_{s, T} \mathbf{F}_s^T \tilde{\mathbf{V}}_s^{-1} \mathbf{y}_{s, 1:T}$.

S5.3 Deep Interweaving

To improve the mixing in the draws of the factor loading matrix we employ the following deep interweaving strategy introduced by Kastner et al. [2017].

- Determine the vector $\boldsymbol{\beta}_{\cdot,k}^*$, where $\beta_{s,k}^* = \beta_{s,k}^{old} / \beta_{k,k}^{old}$ in the k th column of the transformed factor loading matrix $\boldsymbol{\beta}^*$.
- Define $\boldsymbol{\lambda}_{k,\cdot}^* = \boldsymbol{\lambda}_{k,\cdot}^{old} + 2 \log |\beta_{k,k}^{old}|$ and sample $\beta_{k,k}^{new}$ from $p(\beta_{k,k} | \beta_{\cdot,k}^*, \boldsymbol{\lambda}_{k,\cdot}^*, \phi_k, \tau_{f,k}^2)$.
- Update $\boldsymbol{\beta}_{\cdot,k} = \frac{\beta_{k,k}^{new}}{\beta_{k,k}^{old}} \boldsymbol{\beta}_{\cdot,k}^{old}$, $\mathbf{f}_{k,\cdot} = \frac{\beta_{k,k}^{old}}{\beta_{k,k}^{new}} \mathbf{f}_{k,\cdot}^{old}$, and $\boldsymbol{\lambda}_{k,\cdot} = \boldsymbol{\lambda}_{k,\cdot}^{old} + 2 \log \left| \frac{\beta_{k,k}^{old}}{\beta_{k,k}^{new}} \right|$.

In the deep interweaving representation the scaling parameter $\beta_{k,k}$ is sampled indirectly through $\mu_{f,k} = \log \beta_{k,k}^2$, $k = 1, \dots, K$. The implied prior $p(\mu_{f,k}) \propto \exp(\mu_{f,k}/2 - \exp(\mu_{f,k})/2)$ and the density $p(\boldsymbol{\beta}_{\cdot,k}^* | \mu_{f,k}) \sim N_{k_l}(0, \exp(-\mu_{f,k}) I_{k_l})$ and the likelihood yields the posterior

$$p(\mu_{f,k} | \boldsymbol{\beta}_{\cdot,k}^*, \boldsymbol{\lambda}_{k,\cdot}^*, \phi_k, \tau_{f,k}^2) \propto p(\boldsymbol{\lambda}_{k,\cdot}^* | \mu_{f,k}, \phi_k, \tau_{f,k}^2) p(\boldsymbol{\beta}_{\cdot,k}^* | \mu_{f,k}) p(\mu_{f,k}),$$

which is not in recognisable form. We draw a proposal for $\mu_{f,k}^{prop}$ from $N(A, B)$ where

$$A = \frac{\sum_{t=2}^{T-1} \lambda_{k,t}^* + (\lambda_{k,T}^* - \phi_k \lambda_{k,1}^*) / (1 - \phi_k)}{T - 1 + 1/B_0}, B = \frac{\tau_{f,k}^2 / (1 - \phi_k)^2}{T - 1 + 1/B_0}.$$

Denoting the current value $\mu_{f,k}$ by $\mu_{f,k}^{old}$, the new value $\mu_{f,k}^{prop}$ gets accepted with probability $\min(1, R)$, where

$$R = \frac{p(\mu_{f,k}^{prop}) p(\lambda_{k,1}^* | \mu_{f,k}^{prop}, \phi_k, \tau_{f,k}^2) p(\boldsymbol{\beta}_{\cdot,k}^* | \mu_{f,k}^{prop})}{p(\mu_{f,k}^{old}) (\lambda_{k,1}^* | \mu_{f,k}^{old}, \phi_k, \tau_{f,k}^2) p(\boldsymbol{\beta}_{\cdot,k}^* | \mu_{f,k}^{old})} \times \frac{p_{aux}(\mu_{f,k}^{old} | \phi_k, \tau_{f,k}^2)}{p_{aux}(\mu_{f,k}^{prop} | \phi_k, \tau_{f,k}^2)},$$

where

$$p_{aux}(\mu_{f,k}^{old} | \phi_k, \tau_{f,k}^2) \sim N(0, B_0 \tau_{f,k}^2 / (1 - \phi_k)^2).$$

The constant B_0 is set to large value 10^5 as in Kastner et al. [2017].

S5.4 Sampling the Latent Factors $\mathbf{f}_{1:T}$

After some algebra, we obtain that

$$\{\mathbf{f}_t\} | \mathbf{y}, \{\mathbf{h}_t\}, \{\boldsymbol{\lambda}_t\}, \boldsymbol{\beta} \sim N(a_t, b_t), \quad (\text{S20})$$

where $b_t = (\boldsymbol{\beta}^T \mathbf{V}_t^{-1} \boldsymbol{\beta} + \mathbf{D}_t^{-1})^{-1}$ and $a_t = b_t \boldsymbol{\beta}^T \mathbf{V}_t^{-1} \mathbf{y}_t$.

S6 Tables and figures for the factor stochastic volatility model in Sections 4.2.1 and 4.2.2

Table S1: Inefficiency factor of β , α , μ , τ^2 , ϕ , and τ_f^2 with exact transition density for the Gaussian OU model: Sampler I: $PMMH(\alpha, \tau^2, \tau_f^2) + PG(\beta, \mu, \phi)$, Sampler II: $PGAT(\beta, \alpha, \tau^2, \mu, \phi, \tau_f^2)$, sampler III: $PGBS(\beta, \alpha, \tau^2, \mu, \phi, \tau_f^2)$ for simulated data with $T = 1000$, $S = 20$, and $K = 1$, and number of particles $N = 500$.

	I	II	III		I	II	III		I	II	III		I	II	III
β_1	12.55	12.92	13.95	α_1	12.64	66.69	39.94	$\tau_{\epsilon,1}^2$	14.70	136.58	99.80	μ_1	1.29	1.47	1.39
β_2	12.67	13.03	13.94	α_2	11.76	44.67	35.59	$\tau_{\epsilon,2}^2$	14.36	72.64	74.03	μ_2	1.28	1.43	1.33
β_3	12.69	13.20	14.17	α_3	11.89	64.76	61.08	$\tau_{\epsilon,3}^2$	12.01	92.80	101.64	μ_3	1.56	1.72	1.59
β_4	12.53	12.37	13.77	α_4	13.13	107.58	59.69	$\tau_{\epsilon,4}^2$	14.70	283.23	93.35	μ_4	1.41	1.40	1.33
β_5	12.66	13.08	13.86	α_5	15.21	76.45	35.94	$\tau_{\epsilon,5}^2$	14.56	123.53	81.58	μ_5	1.29	1.37	1.25
β_6	12.76	12.89	14.01	α_6	14.80	37.25	30.74	$\tau_{\epsilon,6}^2$	14.84	76.76	56.96	μ_6	1.25	1.29	1.18
β_7	12.56	12.62	13.72	α_7	14.11	27.87	24.29	$\tau_{\epsilon,7}^2$	13.36	58.61	43.39	μ_7	1.23	1.28	1.18
β_8	12.85	12.96	13.87	α_8	13.65	40.08	19.94	$\tau_{\epsilon,8}^2$	13.37	98.49	42.14	μ_8	1.24	1.27	1.20
β_9	12.52	13.11	13.83	α_9	13.58	96.90	47.77	$\tau_{\epsilon,9}^2$	15.06	144.72	81.66	μ_9	1.99	1.86	1.54
β_{10}	12.39	12.81	14.05	α_{10}	18.07	23.49	32.13	$\tau_{\epsilon,10}^2$	16.56	58.06	57.03	μ_{10}	1.29	1.28	1.23
β_{11}	12.80	12.94	14.13	α_{11}	17.31	41.43	31.13	$\tau_{\epsilon,11}^2$	14.33	75.79	66.30	μ_{11}	1.33	1.37	1.27
β_{12}	12.75	13.07	14.22	α_{12}	16.33	30.14	47.93	$\tau_{\epsilon,12}^2$	14.18	53.80	74.84	μ_{12}	1.42	1.35	1.31
β_{13}	12.78	12.87	14.16	α_{13}	16.24	38.37	27.31	$\tau_{\epsilon,13}^2$	13.67	67.67	47.37	μ_{13}	1.25	1.31	1.25
β_{14}	12.78	13.04	14.23	α_{14}	14.41	38.38	21.61	$\tau_{\epsilon,14}^2$	15.88	83.16	46.09	μ_{14}	1.27	1.30	1.26
β_{15}	12.47	12.82	13.80	α_{15}	12.72	34.25	22.16	$\tau_{\epsilon,15}^2$	15.39	60.91	44.90	μ_{15}	1.22	1.25	1.19
β_{16}	12.91	12.99	14.01	α_{16}	15.19	70.11	42.38	$\tau_{\epsilon,16}^2$	13.60	110.75	66.36	μ_{16}	1.40	1.62	1.34
β_{17}	12.74	13.11	13.86	α_{17}	11.17	22.16	27.11	$\tau_{\epsilon,17}^2$	11.43	53.60	51.73	μ_{17}	1.37	1.31	1.21
β_{18}	12.58	12.93	13.84	α_{18}	12.74	28.17	28.51	$\tau_{\epsilon,18}^2$	15.66	59.10	75.58	μ_{18}	1.33	1.32	1.30
β_{19}	12.64	12.81	13.80	α_{19}	12.67	40.38	29.96	$\tau_{\epsilon,19}^2$	15.17	74.87	59.19	μ_{19}	1.44	1.57	1.41
β_{20}	12.77	13.19	14.08	α_{20}	12.85	27.12	22.34	$\tau_{\epsilon,20}^2$	12.84	73.02	44.80	μ_{20}	1.26	1.38	1.30
ϕ	8.03	20.12	18.62	$\tau_{f,1}^2$	14.76	73.76	79.14								

Table S3 gives the inefficiency factors of β , α , μ , τ_ϵ^2 , ϕ , and τ_f^2 with the exact transition density for the Gaussian OU model for the three samplers: Sampler I: $PMMH(\alpha, \tau_\epsilon^2, \tau_f^2) + PG(\beta, \mu, \phi)$, Sampler II: $PGAT(\beta, \alpha, \tau_\epsilon^2, \mu, \phi, \tau_f^2)$, sampler III: $PGBS(\beta, \alpha, \tau_\epsilon^2, \mu, \phi, \tau_f^2)$ for US stock returns data with $T = 1000$, $S = 20$, and $K = 1$, and with the number of particles $N = 500$.

Table S4 gives the inefficiency factors of β , α , μ , τ_ϵ^2 , ϕ , and τ_f^2 with the approximate Euler based transition density for the Gaussian OU model, for the three samplers: Sampler I: $PMMH(\alpha, \tau_\epsilon^2, \tau_f^2) + PG(\beta, \mu, \phi)$, Sampler II: $PGAT(\beta, \alpha, \tau_\epsilon^2, \mu, \phi, \tau_f^2)$, Sampler III: $PGBS(\beta, \alpha, \tau_\epsilon^2, \mu, \phi, \tau_f^2)$ for US stock returns data with $T = 1000$, $S = 20$, and $K = 1$, and with the number of particles $N = 1000$.

Table S2: Inefficiency factor of β , α , μ , τ^2 , ϕ , and τ_f^2 with Euler approximation for state transition density for the Gaussian OU model: Sampler I: $PMMH(\alpha, \tau^2, \mu, \tau_f^2) + PG(\beta, \phi)$, Sampler II: $PGAT(\beta, \alpha, \tau^2, \mu, \phi, \tau_f^2)$, sampler III: $PGBS(\beta, \alpha, \tau^2, \mu, \phi, \tau_f^2)$ for simulated data with $T = 1000$, $S = 20$, and $K = 1$, and number of particles $N = 1000$.

	I	II	III	I	II	III	I	II	III	I	II	III	I	II	III
β_1	13.72	13.67	11.06	α_1	12.85	159.79	181.78	$\tau_{\epsilon,1}^2$	13.10	374.25	444.82	μ_1	13.27	12.92	11.82
β_2	13.93	13.79	11.23	α_2	15.49	92.87	335.05	$\tau_{\epsilon,2}^2$	13.49	340.28	792.88	μ_2	13.42	11.00	11.98
β_3	13.87	13.60	11.30	α_3	12.43	300.77	272.34	$\tau_{\epsilon,3}^2$	12.46	733.43	682.28	μ_3	15.41	13.09	13.23
β_4	14.14	13.48	10.95	α_4	13.35	530.99	303.41	$\tau_{\epsilon,4}^2$	13.46	977.93	654.65	μ_4	13.44	13.87	14.16
β_5	13.63	13.56	10.95	α_5	15.72	93.77	140.44	$\tau_{\epsilon,5}^2$	16.23	514.24	339.73	μ_5	13.24	11.83	12.87
β_6	13.84	13.68	11.30	α_6	16.81	190.71	152.17	$\tau_{\epsilon,6}^2$	16.20	539.97	418.23	μ_6	14.00	13.23	13.45
β_7	13.77	13.69	11.25	α_7	17.57	79.74	102.55	$\tau_{\epsilon,7}^2$	13.75	592.05	352.65	μ_7	13.80	10.85	11.77
β_8	13.87	13.52	11.14	α_8	13.33	134.56	136.97	$\tau_{\epsilon,8}^2$	13.99	392.80	376.86	μ_8	16.46	11.48	11.67
β_9	13.69	13.39	11.15	α_9	13.50	395.91	161.91	$\tau_{\epsilon,9}^2$	14.65	803.36	457.15	μ_9	16.12	13.72	12.55
β_{10}	13.95	13.66	11.19	α_{10}	12.46	128.96	117.10	$\tau_{\epsilon,10}^2$	13.10	408.40	357.97	μ_{10}	14.72	11.70	11.94
β_{11}	13.99	13.84	11.14	α_{11}	13.55	273.87	98.71	$\tau_{\epsilon,11}^2$	15.56	667.52	402.61	μ_{11}	12.55	11.51	12.62
β_{12}	13.85	13.78	11.32	α_{12}	16.34	105.64	204.73	$\tau_{\epsilon,12}^2$	16.09	356.37	438.96	μ_{12}	12.56	13.00	13.25
β_{13}	14.20	13.56	11.13	α_{13}	13.56	262.15	136.41	$\tau_{\epsilon,13}^2$	12.73	511.17	378.67	μ_{13}	13.18	14.97	11.28
β_{14}	14.12	13.92	11.34	α_{14}	12.60	188.22	177.73	$\tau_{\epsilon,14}^2$	12.00	530.42	428.24	μ_{14}	16.19	12.18	11.69
β_{15}	13.65	13.27	11.00	α_{15}	14.79	200.20	162.37	$\tau_{\epsilon,15}^2$	12.79	574.45	578.06	μ_{15}	15.09	13.01	12.46
β_{16}	13.89	13.89	11.07	α_{16}	14.62	271.96	337.69	$\tau_{\epsilon,16}^2$	15.67	470.91	672.67	μ_{16}	13.51	15.99	11.88
β_{17}	13.77	13.30	11.07	α_{17}	16.29	139.51	87.63	$\tau_{\epsilon,17}^2$	13.62	467.94	330.15	μ_{17}	16.63	12.34	13.24
β_{18}	13.71	13.40	10.96	α_{18}	15.69	55.90	107.32	$\tau_{\epsilon,18}^2$	17.08	262.38	317.31	μ_{18}	15.03	10.81	11.65
β_{19}	13.90	13.69	11.05	α_{19}	15.73	284.70	194.08	$\tau_{\epsilon,19}^2$	14.97	649.26	537.12	μ_{19}	15.39	13.53	11.72
β_{20}	13.86	13.61	11.21	α_{20}	13.76	311.20	125.72	$\tau_{\epsilon,20}^2$	14.99	667.49	331.18	μ_{20}	14.64	16.43	15.96
ϕ	7.11	20.88	17.01	$\tau_{f,1}^2$	12.66	78.23	67.92								

Table S3: Inefficiency factors of β , α , μ , τ^2 , ϕ , and τ_f^2 with exact transition density for the Gaussian OU model: Sampler I: $PMMH(\alpha, \tau^2, \tau_f^2) + PG(\beta, \mu, \phi)$, Sampler II: $PGAT(\beta, \alpha, \tau^2, \mu, \phi, \tau_f^2)$, sampler III: $PGBS(\beta, \alpha, \tau^2, \mu, \phi, \tau_f^2)$ for US stock returns data with $T = 1000$, $S = 20$, and $K = 1$, and number of particles $N = 500$.

	I	II	III	I	II	III	I	II	III	I	II	III			
β_1	2.18	2.05	1.91	α_1	14.21	219.61	113.66	$\tau_{\epsilon,1}^2$	14.37	260.88	129.79	μ_1	2.11	4.50	2.84
β_2	1.68	1.85	1.90	α_2	11.87	35.87	40.80	$\tau_{\epsilon,2}^2$	12.29	68.34	70.17	μ_2	1.20	1.42	1.18
β_3	1.80	1.76	1.70	α_3	13.04	62.04	89.69	$\tau_{\epsilon,3}^2$	13.23	110.88	157.46	μ_3	2.39	2.66	2.36
β_4	1.79	1.76	1.83	α_4	14.22	66.24	51.79	$\tau_{\epsilon,4}^2$	14.99	122.26	88.17	μ_4	1.77	1.83	1.50
β_5	1.87	1.76	1.69	α_5	18.44	466.48	136.77	$\tau_{\epsilon,5}^2$	17.14	682.49	167.35	μ_5	2.97	3.57	1.91
β_6	1.66	1.74	1.67	α_6	17.31	113.00	112.08	$\tau_{\epsilon,6}^2$	19.29	202.66	258.42	μ_6	4.88	5.94	4.11
β_7	1.61	1.67	1.66	α_7	11.41	52.72	64.09	$\tau_{\epsilon,7}^2$	14.00	91.79	92.67	μ_7	1.87	1.79	1.86
β_8	1.82	1.93	1.70	α_8	18.71	86.37	45.28	$\tau_{\epsilon,8}^2$	20.57	145.71	76.37	μ_8	2.43	3.41	1.80
β_9	1.89	1.96	1.74	α_9	12.97	80.73	136.71	$\tau_{\epsilon,9}^2$	14.23	116.44	158.23	μ_9	2.27	2.77	3.30
β_{10}	1.65	1.73	1.66	α_{10}	15.25	119.34	124.61	$\tau_{\epsilon,10}^2$	12.54	106.68	128.63	μ_{10}	6.21	7.57	6.70
β_{11}	1.63	1.74	1.67	α_{11}	14.66	65.71	69.71	$\tau_{\epsilon,11}^2$	14.44	121.39	83.53	μ_{11}	3.24	5.57	2.84
β_{12}	1.65	1.89	1.69	α_{12}	17.47	433.51	97.20	$\tau_{\epsilon,12}^2$	16.20	545.21	146.63	μ_{12}	3.36	5.94	2.54
β_{13}	1.94	2.02	1.92	α_{13}	13.50	151.20	112.64	$\tau_{\epsilon,13}^2$	13.49	189.17	145.44	μ_{13}	2.74	3.19	2.19
β_{14}	1.66	1.79	1.60	α_{14}	14.48	70.44	74.94	$\tau_{\epsilon,14}^2$	14.11	146.32	121.04	μ_{14}	2.01	2.06	1.73
β_{15}	1.62	1.82	1.45	α_{15}	13.08	126.39	291.78	$\tau_{\epsilon,15}^2$	14.80	148.03	382.86	μ_{15}	2.20	2.66	2.11
β_{16}	1.69	1.76	1.83	α_{16}	11.58	133.17	39.94	$\tau_{\epsilon,16}^2$	11.64	210.38	99.40	μ_{16}	1.54	1.54	1.55
β_{17}	2.12	2.54	1.95	α_{17}	14.52	39.97	30.94	$\tau_{\epsilon,17}^2$	15.65	94.23	54.03	μ_{17}	1.30	1.25	1.24
β_{18}	1.94	2.04	1.93	α_{18}	15.24	51.58	40.02	$\tau_{\epsilon,18}^2$	17.46	105.41	70.14	μ_{18}	1.36	1.51	1.36
β_{19}	1.80	1.92	1.73	α_{19}	15.14	36.14	28.02	$\tau_{\epsilon,19}^2$	13.73	81.59	68.35	μ_{19}	1.28	1.48	1.37
β_{20}	1.87	1.81	1.73	α_{20}	14.52	33.78	28.57	$\tau_{\epsilon,20}^2$	17.10	72.67	55.28	μ_{20}	1.27	1.51	1.22
ϕ	8.77	25.64	20.05	$\tau_{f,1}^2$	14.24	55.08	48.92								

Table S4: Inefficiency factors of β , α , μ , τ^2 , ϕ , and τ_f^2 with an Euler approximation for the state transition densities for the Gaussian OU model: Sampler I: $PMMH(\alpha, \tau^2, \mu, \tau_f^2) + PG(\beta, \phi)$, Sampler II: $PGAT(\beta, \alpha, \tau^2, \mu, \phi, \tau_f^2)$, sampler III: $PGBS(\beta, \alpha, \tau^2, \mu, \phi, \tau_f^2)$ for US stock returns data with $T = 1000$, $S = 20$, and $K = 1$, and number of particles $N = 1000$.

	I	II	III	I	II	III	I	II	III	I	II	III			
β_1	2.01	2.18	1.89	α_1	15.52	559.41	723.77	$\tau_{\epsilon,1}^2$	15.33	787.45	977.73	μ_1	11.99	23.88	18.17
β_2	1.86	1.84	1.83	α_2	16.40	554.76	186.87	$\tau_{\epsilon,2}^2$	14.35	914.39	475.00	μ_2	15.46	12.34	11.59
β_3	1.80	1.79	1.73	α_3	18.50	342.35	210.83	$\tau_{\epsilon,3}^2$	19.40	688.81	546.86	μ_3	13.45	12.56	12.66
β_4	1.79	1.83	1.76	α_4	15.40	215.12	111.11	$\tau_{\epsilon,4}^2$	16.44	455.87	326.75	μ_4	12.11	12.82	12.83
β_5	1.85	1.75	1.68	α_5	15.82	308.00	305.18	$\tau_{\epsilon,5}^2$	19.29	576.04	456.33	μ_5	21.39	16.70	20.62
β_6	1.73	1.75	1.74	α_6	20.72	494.91	374.78	$\tau_{\epsilon,6}^2$	20.06	995.03	797.53	μ_6	19.43	26.62	36.67
β_7	1.78	1.75	1.77	α_7	16.07	340.91	464.08	$\tau_{\epsilon,7}^2$	14.49	783.92	754.46	μ_7	13.71	13.56	14.80
β_8	1.83	1.83	1.74	α_8	19.85	400.60	128.31	$\tau_{\epsilon,8}^2$	23.81	928.38	328.45	μ_8	18.30	13.56	12.63
β_9	1.76	1.96	1.77	α_9	15.19	909.99	546.01	$\tau_{\epsilon,9}^2$	14.84	1215.77	937.28	μ_9	13.06	19.86	19.14
β_{10}	1.74	1.78	1.77	α_{10}	16.96	385.25	236.04	$\tau_{\epsilon,10}^2$	23.59	962.51	716.08	μ_{10}	11.92	50.67	35.06
β_{11}	1.77	1.78	1.74	α_{11}	18.43	368.53	115.84	$\tau_{\epsilon,11}^2$	23.99	811.02	872.32	μ_{11}	13.76	15.12	14.85
β_{12}	1.81	1.82	1.77	α_{12}	20.48	521.58	460.67	$\tau_{\epsilon,12}^2$	20.43	771.17	700.72	μ_{12}	16.91	20.80	19.88
β_{13}	1.81	1.86	1.83	α_{13}	17.79	362.85	548.70	$\tau_{\epsilon,13}^2$	18.43	632.95	707.42	μ_{13}	15.76	14.73	19.90
β_{14}	1.77	1.79	1.64	α_{14}	15.48	195.27	375.87	$\tau_{\epsilon,14}^2$	17.05	603.04	704.08	μ_{14}	14.14	14.75	19.37
β_{15}	1.59	1.69	1.57	α_{15}	17.48	485.37	1097.26	$\tau_{\epsilon,15}^2$	15.58	897.29	1228.99	μ_{15}	15.76	18.84	29.16
β_{16}	1.80	1.70	1.74	α_{16}	15.94	240.28	211.86	$\tau_{\epsilon,16}^2$	14.50	571.97	434.93	μ_{16}	13.40	13.29	13.19
β_{17}	2.14	2.12	2.02	α_{17}	16.99	143.03	330.84	$\tau_{\epsilon,17}^2$	17.16	496.86	683.20	μ_{17}	15.79	11.49	10.91
β_{18}	1.88	1.96	1.87	α_{18}	18.10	225.30	184.31	$\tau_{\epsilon,18}^2$	16.15	518.71	683.36	μ_{18}	18.81	11.63	12.63
β_{19}	1.84	1.88	1.79	α_{19}	16.61	200.54	70.61	$\tau_{\epsilon,19}^2$	16.24	474.26	276.66	μ_{19}	16.64	11.33	8.73
β_{20}	1.91	1.86	1.77	α_{20}	13.97	94.55	310.15	$\tau_{\epsilon,20}^2$	16.21	306.76	726.35	μ_{20}	17.31	10.68	11.21
ϕ	8.22	22.73	34.20	$\tau_{f,1}^2$	12.36	52.16	68.27								

Figures S1 and S2 present the kernel density estimates of marginal posterior densities of four representative α and τ_ϵ^2 respectively for the Gaussian OU model for the US stock returns data. The density estimates are for PMMH+PG using exact and approximate transition densities and PG with approximate transition densities using ancestral tracing and backward simulation. Both figures show that both PMMH+PG samplers produce estimates that are close to each other, whereas the PG samplers are much less reliable.

Figure S1: The kernel density estimates of marginal posterior densities of four representative α for the US stock returns data. The density estimates are for PMMH+PG using exact and approximate transition densities and PG with approximate transition densities using ancestral tracing and backward simulation for the Gaussian OU model.

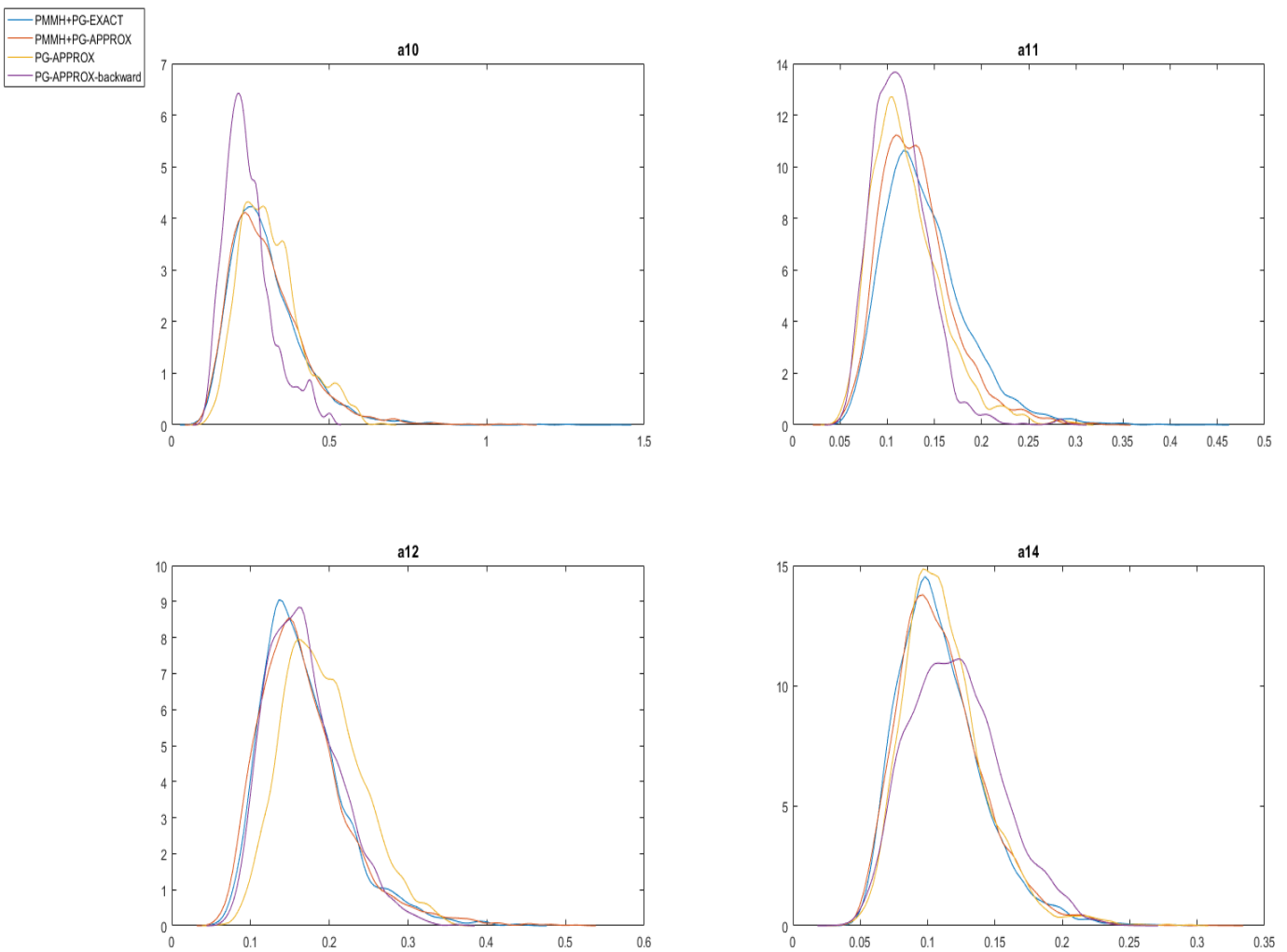


Figure S2: The kernel density estimates of marginal posterior densities of τ_ϵ^2 for the US stock returns data for four representative τ_ϵ^2 . The density estimates are for PMMH+PG using exact and approximate transition densities and PG using ancestral tracing and backward simulation for the Gaussian OU model.

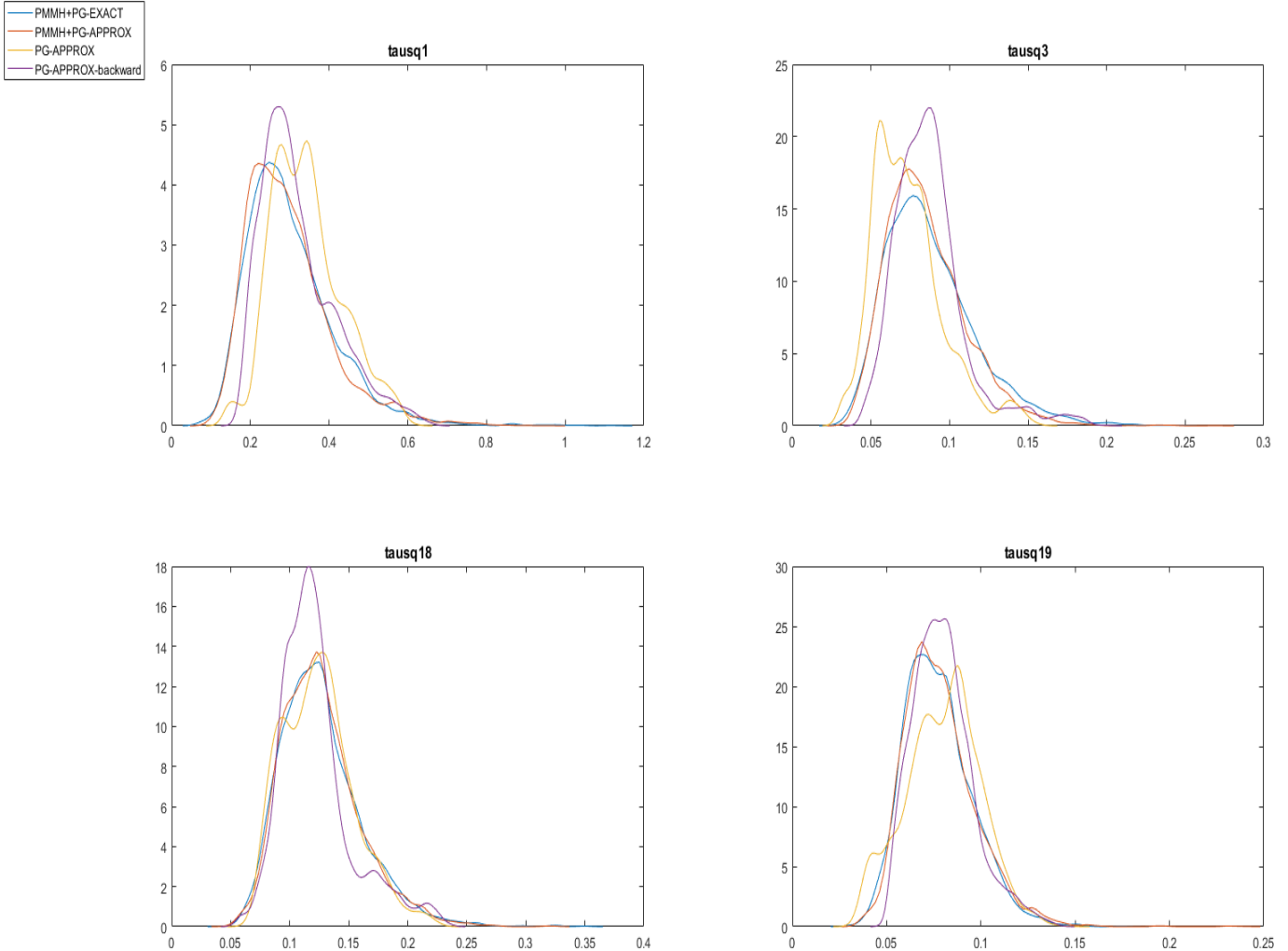


Table S5 gives the inefficiency factors of β , α , μ , τ_ϵ^2 , ϕ , and τ_f^2 with the approximate Euler based transition density for the GARCH diffusion model, for the three samplers: Sampler I: $PMMH(\alpha, \tau_\epsilon^2, \tau_f^2, \mu) + PG(\mathbf{f}_{1:T}, \beta, \phi)$, Sampler II: $PGAT(\mathbf{f}_{1:T}, \beta, \alpha, \tau_\epsilon^2, \mu, \phi, \tau_f^2)$, Sampler III: $PGBS(\mathbf{f}_{1:T}, \beta, \alpha, \tau_\epsilon^2, \mu, \phi, \tau_f^2)$ for US stock returns data with $T = 1000$, $S = 20$, and $K = 1$, and with the number of particles $N = 1000$.

Table S5: Inefficiency factors of β , α , μ , τ^2 , ϕ , and τ_f^2 with an Euler approximation for the state transition densities for the GARCH diffusion model: Sampler I: $PG(\mathbf{f}_{1:T}, \beta, \phi) + PMMH(\alpha, \tau^2, \mu, \tau_f^2)$, Sampler II: $PGAT(\mathbf{f}_{1:T}, \beta, \alpha, \tau^2, \mu, \phi, \tau_f^2)$, sampler III: $PGBS(\mathbf{f}_{1:T}, \beta, \alpha, \tau^2, \mu, \phi, \tau_f^2)$ for US stock returns data with $T = 1000$, $P = 20$, and $K = 1$, and number of particles $N = 1000$.

	I	II	III	I	II	III	I	II	III	I	II	III			
β_1	1.91	2.06	1.88	α_1	32.83	197.50	318.60	τ_1^2	48.24	1944.73	1079.01	μ_1	111.02	207.54	229.44
β_2	1.73	1.77	1.76	α_2	13.31	144.70	135.32	τ_2^2	12.39	2186.34	2205.98	μ_2	14.57	227.46	130.33
β_3	1.69	1.76	1.72	α_3	13.53	179.77	186.45	τ_3^2	23.59	1794.07	654.43	μ_3	19.46	212.72	143.36
β_4	1.70	1.77	1.76	α_4	14.94	225.04	157.04	τ_4^2	16.84	3098.27	1208.39	μ_4	23.45	163.81	118.05
β_5	1.71	1.74	1.71	α_5	16.23	420.88	421.26	τ_5^2	14.29	558.61	3257.52	μ_5	19.34	322.81	243.11
β_6	1.66	1.72	1.68	α_6	18.66	875.82	1166.83	τ_6^2	21.67	1097.21	2746.64	μ_6	18.93	359.97	638.61
β_7	1.64	1.73	1.66	α_7	14.81	488.09	447.91	τ_7^2	16.79	1932.45	2415.33	μ_7	35.95	247.08	205.50
β_8	1.75	1.86	1.72	α_8	18.77	180.04	152.92	τ_8^2	17.51	681.34	2236.32	μ_8	16.08	140.56	231.74
β_9	1.76	1.79	1.85	α_9	23.51	655.71	543.04	τ_9^2	23.17	2465.44	3065.63	μ_9	147.16	434.49	814.62
β_{10}	1.70	1.77	1.75	α_{10}	13.04	1159.77	969.04	τ_{10}^2	14.04	2013.82	1638.88	μ_{10}	17.20	902.78	322.78
β_{11}	1.69	1.77	1.74	α_{11}	11.05	298.47	210.95	τ_{11}^2	14.72	1224.84	2551.95	μ_{11}	17.49	335.21	216.52
β_{12}	1.68	1.86	1.78	α_{12}	19.20	462.64	495.65	τ_{12}^2	22.52	2865.97	1412.81	μ_{12}	49.95	179.47	351.02
β_{13}	1.78	1.85	1.86	α_{13}	14.12	232.22	270.89	τ_{13}^2	13.88	1646.83	2770.24	μ_{13}	16.15	230.03	597.87
β_{14}	1.61	1.63	1.63	α_{14}	17.59	159.37	337.67	τ_{14}^2	16.22	2651.10	1083.02	μ_{14}	15.34	146.47	227.23
β_{15}	1.54	1.54	1.52	α_{15}	13.93	330.76	329.03	τ_{15}^2	16.10	1551.35	1303.25	μ_{15}	30.23	164.37	182.29
β_{16}	1.67	1.69	1.62	α_{16}	17.17	352.23	275.77	τ_{16}^2	15.05	2166.59	1121.20	μ_{16}	11.35	141.30	246.14
β_{17}	2.04	2.16	2.03	α_{17}	16.20	202.76	198.07	τ_{17}^2	17.68	2007.36	3053.61	μ_{17}	36.97	728.55	820.53
β_{18}	1.83	1.86	1.77	α_{18}	13.94	347.07	192.65	τ_{18}^2	17.27	1478.12	2889.07	μ_{18}	19.63	311.89	603.94
β_{19}	1.74	1.80	1.78	α_{19}	14.17	398.65	157.60	τ_{19}^2	18.14	2896.07	2682.24	μ_{19}	19.85	1340.20	235.55
β_{20}	1.75	1.81	1.80	α_{20}	17.59	130.58	262.31	τ_{20}^2	15.98	2096.28	1352.18	μ_{20}	17.63	119.10	148.03
ϕ	8.74	21.52	20.91	τ_f^2	13.65	47.47	46.10								